Archaeological and Anthropological Sciences (2019) 11:6785–6802
https://doi.org/10.1007/s12520-019-00937-x

ORIGINAL PAPER

Amphora production in the Guadalquivir valley (Spain) during the Late Roman period: petrographic, mineralogical, and chemical characterization of reference groups

Leandro Fantuzzi[1,2] · Miguel Ángel Cau Ontiveros[2,3,4]

Received: 18 June 2019 / Accepted: 6 September 2019 / Published online: 24 October 2019

Abstract

This paper presents a scientific analysis of Late Roman amphorae from four kiln sites located in the Guadalquivir river basin: Azanaque-Castillejo (AZ), Isla de la Barqueta (IB), Las Monjas-Soto del Rey (SR), and Picachos (PIC). This region was a significant producer and exporter of oil in the Roman Empire and also during the Late Roman period. The amphorae analyzed belong to type Dressel 23 and were used for trading oil to other Mediterranean regions. A total of 36 amphora samples were analyzed by using a combination of instrumental analytical techniques, including thin-section optical microscopy, X-ray diffraction, and X-ray fluorescence, in order to establish reference groups based on the petrographic, mineralogical, and chemical characterization of the materials. The amphorae from the four kiln sites showed approximately similar petrographic fabrics and chemical compositions, as well as strong technological similarities. However, there are slight petrographic and/or chemical differences that allowed for the differentiation of three reference groups (AZ, SR, and IB-PIC). These groups were also compared with existing reference groups for Early Roman amphorae in the same area, and compositional differences were also observed. This is the first time that compositional reference groups for Late Roman amphora kiln sites in the Guadalquivir valley are characterized. Hence, the results of this research not only contribute new evidence on the study of oil amphora production in this region, but they will also serve as a basis for the identification and sourcing of these amphorae in consumption sites and, consequently, for a better understanding of trade networks during the Late Roman period.

Keywords Amphorae · Late Roman · Baetica · Petrography · XRF · XRD

Introduction

During the Roman period, the Guadalquivir valley, in the Roman province of *Baetica* (currently southern Spain), was an area with high industrial production of oil for export to other parts of the Empire. This commercial activity is well documented in several archeological sites across the Mediterranean, especially through the findings of Early Roman oil amphorae, in particular of type Dressel 20, whose production is attested in about 100 kiln sites located in the area between *Hispalis*/Sevilla, *Corduba*/Córdoba, and *Astigi*/Écija (Bonsor 1931; Ponsich 1974, 1979, 1991; Remesal 1977, 1983, 2004; Chic and García Vargas 2004; Berni 2008; Berni and García Vargas 2016). Production and export of oil from this area continued, at a relatively lower scale, in the Late Roman period, as shown by archeological evidence both from production sites (Remesal 1991, 2004; Chic and García Vargas 2004; Berni and Moros 2012, 2017) and from consumption sites (Beltrán 1970; Manacorda 1977; Keay 1984; Reynolds 1995, 2010; Berni 1998; Remolà 2000; Carreras 2014).

Trade of oil from the Guadalquivir valley in Late Roman times was carried out mainly through amphorae of type Dressel

✉ Leandro Fantuzzi
leandro.fantuzzi@uca.es

[1] Departamento de Historia, Geografía y Filosofía, Facultad de Filosofía y Letras, Universidad de Cádiz, Av. Dr. Gómez Ulla 1, 11003 Cádiz, Spain

[2] ERAAUB, Departament d'Història i Arqueologia, Facultat de Geografia i Història, Universitat de Barcelona, c/Montalegre 6-8, 08001 Barcelona, Spain

[3] ICREA, Pg. Lluís Companys 23, 08010 Barcelona, Spain

[4] Centre Camille Jullian, UMR 7299, MMSSH, Aix-en-Provence, France

23, a smaller container than its predecessor type Dressel 20. According to Remesal (1983, 1989, 1991), Dressel 23 amphorae were manufactured in almost 20 workshops along the Guadalquivir valley and its main tributary, the Genil, although only in few of them, there is clear archeological evidence of Late Roman production so far (Fig. 1) (Remesal 1983, 2004; Berni 1998; Romo and Vargas 2001; Chic and García Vargas 2004; Berni and Moros 2012, 2017). Recent field survey by Bourgeon (2016, 2017) documented significant production of Dressel 23 amphorae in the lower Genil valley, where 17 kiln sites were identified. Dressel 23 amphorae from the Guadalquivir and Genil valleys correspond mostly to the variant Dressel 23a (Berni 1998; Berni and Moros 2017; Bourgeon 2017; Fantuzzi and Cau 2017). It is generally accepted that Dressel 23a, which starts to be produced at the end of the third century, derives from the latest variants of Dressel 20, both sharing important morphological and technical features (Remesal 1983; Berni 1998; Bernal 2001; García Vargas and Bernal 2008; Berni and Moros 2017).

Besides these Dressel 23 amphorae produced in the Guadalquivir valley, other amphorae of the same type but mainly related to a different variant (Dressel 23d), also for export of oil, were manufactured in the Baetican coast, in particular in the province of Málaga (Baldomero et al. 1997; Bernal 1997, 2001; Rodríguez 1997; Serrano 2004; García Vargas and Bernal 2008; Corrales et al. 2011). Recent archaeometric studies enabled the characterization of Dressel 23 from Málaga and their differentiation from those produced in the Guadalquivir valley (Fantuzzi and Cau 2017). Production of these amphorae in the Baetican coast started later than in the Guadalquivir valley, around the late fourth century, but, in any case, products from both areas seem to have coexisted, especially during the fifth century (Remolà 2000).

Even if the general characteristics of shape and macroscopic fabric may allow for the identification of Dressel 23 from the Guadalquivir area in consumption sites, this can be done in a fairly generic way, since it has not been possible so far to distinguish fabrics from different workshops or, at least, to get a general idea of the variety of workshops represented in consumption sites. In this regard, the study of oil trade from the Guadalquivir in the Late Roman period is constrained due to a

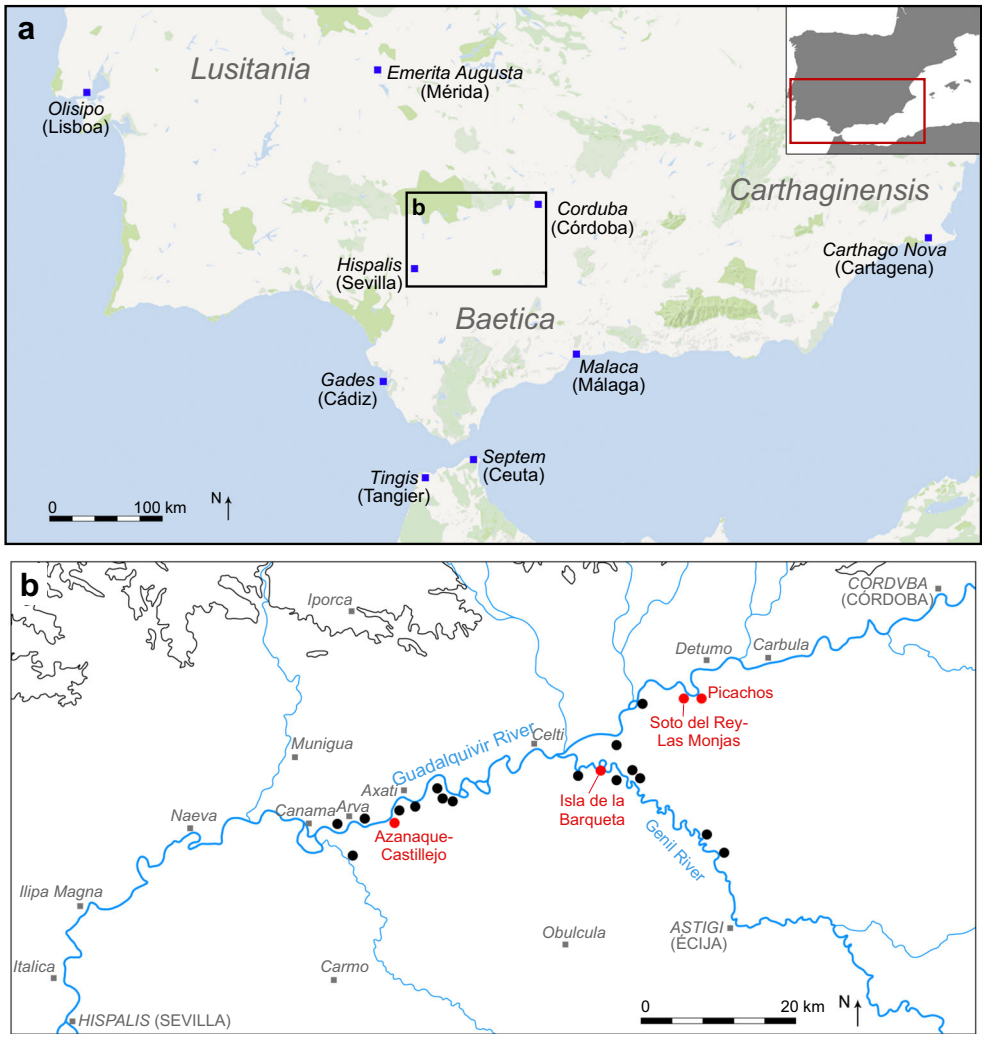

Fig. 1 **a** Location of the middle Guadalquivir valley and the Genil valley in the context of Roman *Baetica*, southern Spain (map data: Google, Instituto Geográfico Nacional). **b** Map of the study area, showing the four kiln sites analyzed in this paper (red dots) and other sites producing amphorae Dressel 23 according to Remesal (1983, 2004; cf. Bourgeon 2017) (black dots)

series of problems. One of these is the notable scarcity of epigraphic evidence on Dressel 23 amphorae, with rare exceptions (Remesal 1983; Chic 1985; Berni 1998, 2008; Berni and Moros 2012, 2017). This contrasts with the situation of the amphora type Dressel 20, with very abundant epigraphic evidence that facilitates its identification in consumption sites and, in many cases, the attribution to a specific workshop (Rodríguez Almeida 1984; Chic 1985, 2001; Blázquez and Remesal 1999, 2001, 2003, 2007, 2010, 2016; Étienne and Mayet 2004; Berni 2008). Another problem is that Dressel 23 amphorae from the Guadalquivir valley tend to show finer fabrics than those of the earlier type Dressel 20 (Berni 1998; Bourgeon 2017), making it more difficult to identify fabrics from different workshops on a macroscopic basis. In fact, in some cases, the macroscopic fabric resembles the one found in some Late Roman Tunisian amphorae (Berni 1998; Viegas 2011), which sometimes may lead to misclassifications. Finally, a significant problem is the lack of published studies on the archaeometric characterization of amphorae produced in the Late Roman kiln sites of the Guadalquivir area. So far, there exist only few compositional studies of Early Roman amphorae from this area (Grubessi 1999; Grubessi and Conti 1999; González Vílchez et al. 2001; Polvorinos del Río et al. 2003; Costa et al. 2012).

In order to start filling this knowledge gap, the aim of this work is to carry out a compositional and technological characterization of Dressel 23 amphorae from selected kiln sites in the Guadalquivir region and, on this basis, to establish reference groups for each of them. In addition to the characterization of the materials, the possible existence of petrographic, mineralogical, and/or chemical markers that could help to differentiate the products from each workshop is also examined. In this way, the research aims at providing new foundations for the study of interregional trade of products transported in amphorae from southern Spain in the Late Roman period, through the definition of reference groups for production sites at this specific area that could be used in the future for comparison with similar materials found in consumption sites across the Mediterranean.

Archeological contexts and geological background

The amphorae selected for this study come from four production sites: Azanaque-Castillejo (AZ), Isla de la Barqueta (IB), Las Monjas-Soto del Rey (SR), and Picachos (PIC).[1] They are all located in the Guadalquivir valley between Sevilla and Córdoba, except for Isla de la Barqueta that is located in the lower Genil valley, very close to the confluence of both rivers (Fig. 1). None of these sites has been excavated up to now, although some kilns were excavated in Castillo de Azanaque, very close to Azanaque-Castillejo (Romo and Vargas 2001; Berni 2008). Nevertheless, in these sites, large accumulations of overfired amphorae, bricks and tiles, as well as rests of kilns, have provided archeological evidence of pottery production from the Early Roman Imperial period—Dressel 20 type—to the Late Roman period—Dressel 23 type (Ponsich 1979; Chic 1985; Berni 2008; Berni and Moros 2012).

The area where the sites are located, that is, the Guadalquivir basin, between Córdoba and Sevilla, is characterized by a complex and heterogeneous geological background (Fig. 2). The basin receives contribution, on one hand, of various Paleozoic (Hercynian) metamorphic, igneous, and sedimentary rocks from the Sierra Morena, the southern end of the Hesperian (or Iberian) Massif. On the other hand, the basin receives Mesozoic and Cenozoic sedimentary materials from the external zones of the Baetic Cordillera (Subbaetic System and Intermediate Units) located to the south of the basin; these include marls, limestones, and sandstone, among others. The depression that forms the Guadalquivir basin is mostly filled with Oligocene and Mio-Pliocene marine sediments, including sandstones, siltstones, marls, and clays, in addition to recent Quaternary deposits (IGME 1970, 1980; Vera 1983; Sala 1984; Junta de Andalucía 1998; González-Delgado et al. 2004).

Materials and methods

Thirty-six amphorae (BET-1 to BET-36) of type Dressel 23 from the four production sites (AZ, IB, SR, and PIC) were sampled for scientific analysis (Table 1; Fig. 3). The sherds, mostly rims and body fragments, were collected from the surface, due to the lack of archeological excavations in these sites so far. All the rim sherds correspond to the variant Dressel 23a / Keay 13A of the type (Berni 1998; Berni and Moros 2017). Macroscopically, they show compact fabrics, with colors ranging from beige-yellow to pinkish or red-orange, usually with a beige-yellow surface. The samples from AZ show a red to orange color to the naked eye, although with a gray core in BET-35 or an almost complete gray section in BET-34. Conversely, samples from the other three kiln sites show colors from beige-yellow to pinkish or, less frequently, red-orange, with variations in the same site and even in the same individuals in some cases. The samples contain not only small and heterogeneous inclusions, mostly colorless and white, but also dark and reddish ones; the presence of quartz and micas can be inferred from the macroscopic observation (Berni and Moros 2012).

[1] The exact locations of these sites, based on the geographic coordinates reported by Chic (2001), are as follows: AZ, 37° 37′ 11.4″ N 5° 33′ 05.9″ W; IB, 37° 41′ 23.6″ N 5° 15′ 16.9″ W; SR, 37° 46′ 29.27″ N 5° 08′ 49.73″ W; PIC, 37° 46′ 05.62″ N 5° 06′ 42.36″ W.

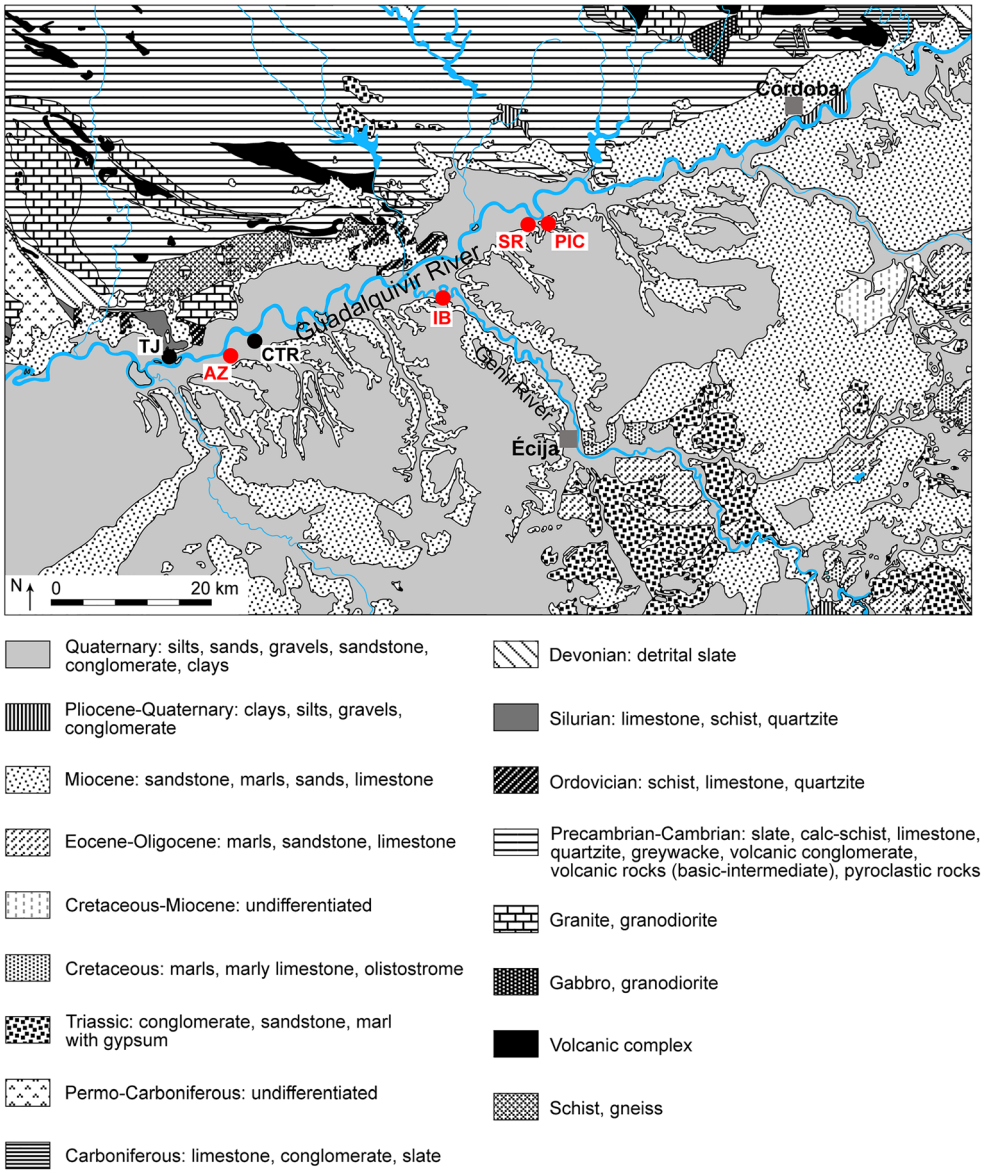

Fig. 2 Geological map of the study area, with the location of the four production sites analyzed (red dots: AZ Azanaque-Castillejo, IB Isla de la Barqueta, SR Las Monjas-Soto del Rey, PIC Picachos) and other sites mentioned in the text (black dots: CTR La Catria, TJ El Tejarillo) (based on IGME 1980)

The amphora samples were analyzed by means of optical microscopy (OM) through thin section analysis for their petrographic-mineralogical characterization, X-ray diffraction (XRD) for obtaining additional data on the mineralogical composition, and wavelength dispersive X-ray fluorescence (WD-XRF) for chemical characterization (Table 1).

OM petrographic-mineralogical analysis of thin sections was performed using an Olympus BX41 polarizing microscope, equipped with a digital camera Olympus DP-70, and working between × 20 and × 200 of magnification. For preparing the thin sections, each amphora sample was impregnated with epoxy resin, mounted using Loctite UV glue and sectioned with a Struers Discoplan TS. The thin sections were finished by hand using a powder abrasive until reaching a thickness of 30 μm in which quartz presents a gray-white first-order interference color. For the study of the petrographic fabrics, the methodology proposed by Whitbread (1989, 1995) and Quinn (2013) was followed. Grain-size classification of the inclusions in the petrographic descriptions was based on the Udden-Wentworth scale.

For XRD and XRF analyses, a sample of each amphora was powdered and homogenized in a tungsten carbide mill and dried at 100 °C for 24 h. XRD measurements were taken using a PANalytical X'Pert PRO MPD alpha 1 diffractometer, working with the Cu Kα radiation (l = 1.5406 Å). Spectra were taken from 5 to 80° 2θ, using a step-size of 0.026° 2θ and a step time of 47.5 s. The evaluation of crystalline phases was carried out using the software HighScore Plus by PANalytical, which includes the Joint Committee of Powder Diffraction Standards (JCPDS) data bank. The crystalline phases identified in each diffractogram, including primary phases and any eventual firing and/or postdepositional phase,

Table 1 List of the amphora samples analyzed from Dressel 23 production sites in the Guadalquivir and lower Genil valleys

Sample	Kiln site	Part of amphora	XRF	XRD	OM
BET-1	Azanaque-Castillejo	Rim	X	X	X
BET-2	Azanaque-Castillejo	Rim	X	X	X
BET-3	Azanaque-Castillejo	Rim	X	X	X
BET-4	Picachos	Rim	X	X	X
BET-5	Picachos	Rim	X	X	X
BET-6	Isla de la Barqueta	Rim	X	X	X
BET-7	Isla de la Barqueta	Rim	X	X	X
BET-8	Soto del Rey-Las Monjas	Rim	X	X	X
BET-9	Soto del Rey-Las Monjas	Rim	X	X	X
BET-10	Picachos	Body	X	X	X
BET-11	Picachos	Body	X	X	X
BET-12	Picachos	Rim	X	X	X
BET-13	Picachos	Rim-handle	X	X	X
BET-14	Picachos	Body	–	–	X
BET-15	Picachos	Body	–	–	X
BET-16	Isla de la Barqueta	Body	X	X	X
BET-17	Isla de la Barqueta	Handle	X	X	X
BET-18	Isla de la Barqueta	Body	X	X	X
BET-19	Isla de la Barqueta	Rim	X	X	X
BET-20	Isla de la Barqueta	Base	X	X	X
BET-21	Isla de la Barqueta	Rim	X	X	X
BET-22	Isla de la Barqueta	Body	X	X	X
BET-23	Isla de la Barqueta	Body	–	–	X
BET-24	Soto del Rey-Las Monjas	Body	X	X	X
BET-25	Soto del Rey-Las Monjas	Body	X	X	X
BET-26	Soto del Rey-Las Monjas	Body	X	X	X
BET-27	Soto del Rey-Las Monjas	Body	X	X	X
BET-28	Soto del Rey-Las Monjas	Body	X	X	–
BET-29	Soto del Rey-Las Monjas	Rim	X	X	X
BET-30	Soto del Rey-Las Monjas	Rim	–	–	X
BET-31	Soto del Rey-Las Monjas	Body	–	–	X
BET-32	Soto del Rey-Las Monjas	Body	–	–	X
BET-33	Azanaque-Castillejo	Rim	X	X	X
BET-34	Azanaque-Castillejo	Rim	X	X	X
BET-35	Azanaque-Castillejo	Rim	X	X	X
BET-36	Azanaque-Castillejo	Rim	X	X	X

were used for the estimation of equivalent firing temperatures (EFT) (Roberts 1963; Maggetti 1982; Murad and Wagner 1996; Cultrone et al. 2001; Buxeda and Cau 2004; Maggetti et al. 2011).

The chemical composition of the amphorae was determined through WD-XRF, using a Panalytical-Axios PW 4400/40 spectrometer. Part of the powdered specimen of each amphora sample was used to prepare, on one hand, fused beads for the determination of major and minor elements, using 0.3 g of specimen in an alkaline fusion with lithium tetraborate (1/20 solution). On the other hand, pressed pellets were prepared for the determination of trace elements, using 5 g of specimen mixed with Elvacite agglutinating, placed over boric acid in an aluminum capsule and pressed during 60 s at 200 kN. Sixty International Geological Standards were used for calibration. The concentrations of 29 major, minor, and trace elements were obtained: Fe_2O_3 (as total Fe), Al_2O_3, MnO, P_2O_5, TiO_2, MgO, CaO, Na_2O, K_2O, SiO_2, Ba, Rb, Mo, Th, Nb, Pb, Zr, Y, Sr, Sn, Ce, Co, Ga, V, Zn, W, Cu, Ni, and Cr. Some of these elements were not included in the statistical analysis, particularly Mo, Sn, and W for their low counting statistics (see Hein et al. 2002) and Co and W due to possible contamination from the tungsten carbide cell of the mill used to prepare the samples. The loss on ignition (LOI) was estimated by heating 0.3 g of dried specimen at 950 °C for 3 h. For multivariate statistical treatment of the chemical data, the chemical concentrations were transformed into additive log-ratios (alr), following the methodology proposed by Aitchison (1986, 2005) and Buxeda (1999).

Results and discussion

Petrographic analysis (OM)

Thin section analysis revealed the presence of approximately similar fabrics in the four workshops analyzed. These were relatively fine grained fabrics, with well to moderately sorted inclusions (10–15%), dominantly silt to very fine sand (< 0.125 mm), and, to a lesser degree, fine sand (0.125–0.25 mm) (Fig. 4a). Coarser inclusions could be present, but usually subordinated to the fraction below 0.25 mm. Textural variations were observed, since in all the workshops analyzed, there were samples with few to common medium sand, as well as rare cases in which medium sand inclusions were frequent (BET-2 and BET-33 from AZ, BET-15 from PIC, and BET-22 from IB). Inclusions in the size range from coarse sand to granules were always rare or very rare.

The inclusions consisted of dominant micritic calcite, calcareous microfossils, and monocrystalline quartz, mostly angular to subrounded (Fig. 4b). The microfossils included ostracods and foraminifera (globigerinids mainly), as well as very rare echinoids. There were also common to few polycrystalline quartz and metamorphic rock fragments, most probably derived from quartz-mica schist and/or phyllite, sometimes with a crenulated texture; rare to very rare metagranitoid fragments were observed, as well as very rare quartz-epidote schist (in BET-5 and BET-11, from PIC). Micas were common to few and consisted of both muscovite and biotite; they were observed as very thin and short laths, usually < 0.05/0.10 mm, but few to rare coarse aggregates of biotite were present as well. Common to few, alkali feldspar was also observed, in addition to few-very few plagioclase and occasional

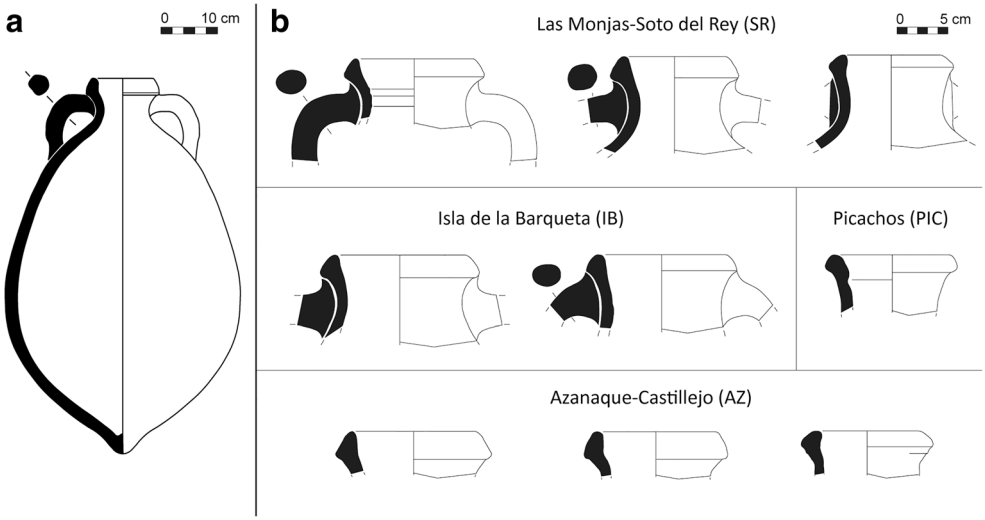

Fig. 3 **a** Representative drawing of Dressel 23a amphora type (from Berni 1998). **b** Examples of Dressel 23 amphora rims from the four kiln sites analyzed in this work (SR and IB from Berni and Moros 2012)

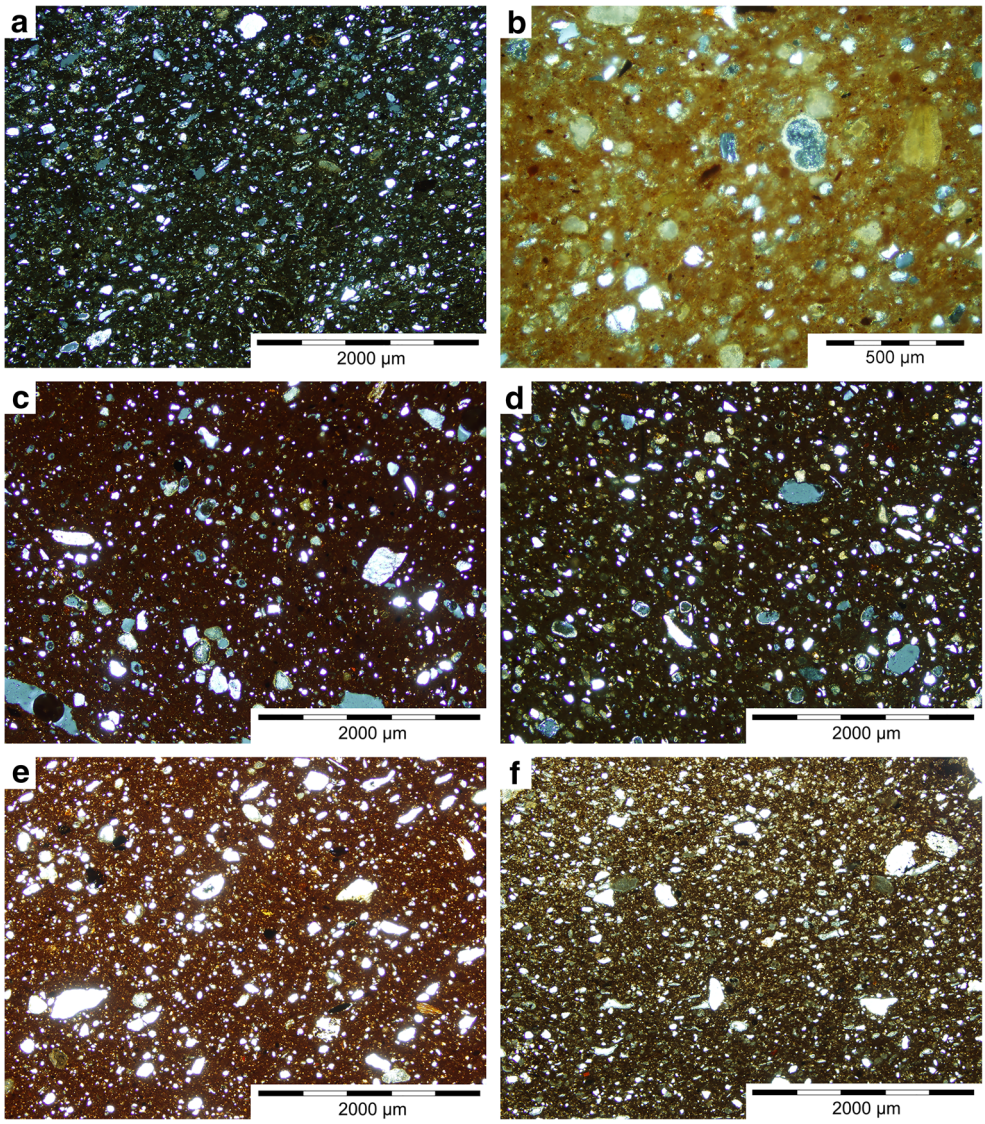

Fig. 4 Photomicrographs of ceramic thin sections, taken under crossed polars (**a**–**d**) or plane polarized light (**e**–**f**). **a** Sample BET-16, from IB, at × 40. **b** Sample BET-27, from SR, at × 100. **c** Sample BET-1, from AZ, at × 40. **d** Sample BET-9, from SR, at × 40. **e** Sample BET-3, from AZ, at × 40. **f** Sample BET-5, from PIC, at × 40

fragments of quartz-sandstone. As accessory—rare to very rare—inclusions, it was possible to find amphibole, epidote, chert (including very rare radiolaria), perthite, clinopyroxene, garnet (except in SR), tourmaline (except in AZ), olivine (only in one sample from AZ), and zircon (in one sample from SR). Very rare fragments of volcanic rocks—probably basalt or andesite—were seen in a few samples from AZ (BET-2 and BET-34), PIC (BET-5 and BET-15), and IB (BET-21).

The main difference that was observed in thin section between samples from distinct workshops concerned the characteristics of the clay matrix and the frequency of carbonate inclusions, which were different in the samples from AZ compared with those from IB, SR, and PIC. Carbonate inclusions—microfossils and calcite—were dominant in all the cases but were even more abundant in the samples from IB, SR, and PIC than in those from AZ (Fig. 4c, d). This difference could be associated with the use of a more calcareous clay paste in IB, SR, and PIC, as suggested also by the characteristics of the clay matrix. The only exception was sample BET-19 from IB, in which the frequency of carbonate inclusions was comparable to that in samples from AZ.

In AZ, the matrix showed a red to reddish brown color in plane polarized light—PPL—(Fig. 4e), except BET-33 and BET-34 with a brown to brown-gray core probably due to firing conditions. Streaks and pellets of two types of clay (a reddish clay and a yellowish-brown one) were observed in few AZ samples (BET-35 and BET-36), which might suggest possible clay mixing. Conversely, in IB, SR, and PIC, the clay matrix showed a brown to yellowish or orange color in PPL (Fig. 4f), in some cases with variations within a same individual. Few, heterogeneous clay streaks and pellets were observed (more in SR than in PIC or IB), although in these cases, it was difficult to ascertain if they were due to natural heterogeneities of the raw clay or to clay mixing. In all the amphorae from the four workshops, the clay matrix was optically inactive, except in two samples from PIC (BET-4 and BET-11) which showed a slightly optically active matrix.

Based on the characteristics of the matrix and inclusions, the amphorae from the four kiln sites analyzed could be associated with the use of marine sedimentary raw clays, with a higher calcareous composition in the case of IB, SR, and PIC, where a marly clay was probably used. Marls and other marine sediments are very abundant throughout the Guadalquivir basin, especially not only on the southern bank, where the four kiln sites are located, but also on the northern bank (Fig. 2). This suggests that the clayey raw materials could have been obtained from the vicinity of the workshops. In the case of AZ, located a bit farther than the other three sites, a more distinct raw clay was used, with a lower content in carbonate inclusions but still with a variety of microfossils that indicates a sedimentary marine origin as well. The presence of metamorphic rocks in the fabrics of the four sites, as well as the very rare presence of volcanic rocks, was also compatible with the local geology, especially with the northern side of the basin where strong contribution from the Sierra Morena is observed (Fig. 2).

The high frequency of fine sand and, in some cases, medium sand inclusions, along with the higher frequency of polycrystalline quartz and metamorphic rock fragments in these grain size ranges than in the finest ones, might suggest the hypothesis that a fine-medium sandy temper was added. However, calcite, microfossils, and quartz were still dominant in this sandy fraction and they could also correspond to natural inclusions in the clayey raw material. For this reason, the hypothesis of a poor refining during the processing of a coarse-textured raw clayey sediment seems plausible.

Except for the lower abundance of carbonate inclusions in AZ, the frequency and nature of other inclusions were rather similar in the four workshops and showed the same range of variability in all of them. The textural variations observed were the result of gradual variability, and they were documented in each of the four sites analyzed.

The porosity was also similar in the fabrics from the four kiln sites. Voids were common but small sized mainly (micro- and meso-sized vesicles and vughs), while few-rare macrovughs and elongated voids with a subparallel orientation to the ceramic walls were also present.

Mineralogical analysis (XRD)

Further information on the mineralogical composition of the amphorae was obtained by means of XRD analysis.

The samples from AZ contained, in all cases, typical firing phases of calcareous ceramic materials (i.e., gehlenite, diopside, plagioclase) and also illite-muscovite, which indicated that the equivalent firing temperature (EFT) could be estimated in the range between 850 and 950 °C. However, there were differences in the intensity of these phases and a gradual evolution of firing temperatures could be inferred: from a sample with small reflections of gehlenite (BET-36; Fig. 5a) to samples with a higher intensity of gehlenite and low of diopside (BET-1, BET-3, and BET-35; Fig. 5b) and, finally, samples with a much higher intensity of diopside and plagioclase, while smaller peaks of gehlenite were still present (BET-2, BET-33 and BET-34: Fig. 5c). Intense peaks of hematite were usually observed, accounting for the reddish macroscopic color of these amphorae. An exception was BET-34, which was the only AZ sample with a gray color to the naked eye and showed much lower content in hematite in XRD, compared with others with the same range of firing temperature and a red color of the fabric; this indicated that the difference in color was partially related to the firing atmosphere in each case. The color of the matrix in samples fired under oxidizing conditions (red colored) from AZ did not show important variations, but in higher-fired samples (Fig. 5c), textural changes were seen, due to decomposition of carbonate inclusions. In these higher-fired samples, small peaks of calcite are still present in the

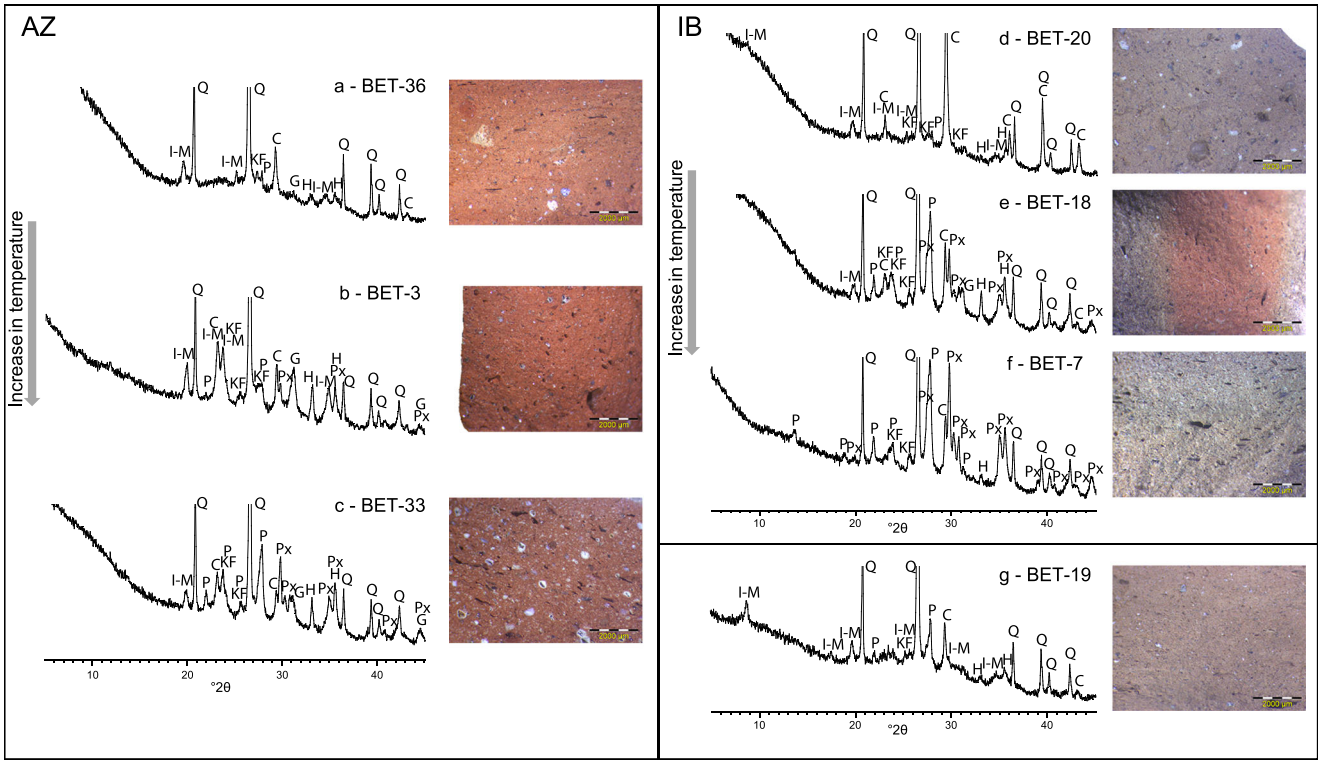

Fig. 5 XRD spectra for selected samples from AZ (a–c) and IB (d–g), and photographs of each individual taken at 15×. Abbreviations for minerals: Q quartz, P plagioclase, KF alkali feldspar, C calcite, G gehlenite, Px pyroxene, H hematite, I-M illite-muscovite

XRD patterns, probably due to recarbonation (as secondary calcite) or, in some cases, due to incomplete decomposition.

A highest variability in the range of firing temperatures was observed in the amphorae from IB and PIC kiln sites. In the case of IB, three main categories could be established: samples with dominant calcite and quartz and small reflections of illite-muscovite (BET-20: Fig. 5d); samples with clear firing phases, in particular diopside, plagioclase, and—in minor amount—gehlenite, and also primary phases including illite-muscovite (BET-6, BET-16, BET-17, BET-18 and BET-21: Fig. 5e); and, finally, samples with total decomposition of illite-muscovite and very intense reflections of diopside and plagioclase (BET-7 and BET-22: Fig. 5f). The estimated EFT should be ≤ 800/850 °C in the first category, 850–950 °C in the second one, and over 950/1000 °C in the third category. The sample BET-19 was another low-fired amphora (EFT ≤ 800/850 °C) but with a lower calcareous composition, showing smaller reflections of calcite and higher of phyllosilicates than in BET-20 (Fig. 5g). Textural changes in the matrix and inclusions were observed to the naked eye in the samples from IB, which were associated with this evolution of firing temperatures (Fig. 5d–f). The color was, in general, beige-yellow (with hue variations), although a few samples presented a red-orange color in the core (BET-6 and BET-18) or walls (BET-17); these latter showed a higher development of hematite in their XRD spectra, which indicated that this color may be related to firing under more oxidizing conditions.

Similar variations in the mineral phase associations to those of IB were found in the samples from PIC. These were associated with the same evolution of equivalent firing temperatures (EFT), that is, below 800/850 °C in samples BET-4 and 11 (Fig. 6a), between 850 and 950 °C in samples BET-5 and BET-10 (Fig. 6b), and over 950/1000 °C in samples BET-12 and BET-13 (Fig. 6c). The macroscopic color of the fabric varied from beige-yellow in the amphorae with the lowest EFT to a heterogeneous color between pinkish and beige-yellow in those with the highest EFT (Fig. 6a–c); in all the cases, the XRD spectra showed very low peaks of hematite.

A different situation was observed in the case of SR. All the amphorae analyzed from this workshop revealed very similar diffractograms, both for the phases that were present and for the intensity of each phase (Fig. 6d). In all these samples, there was a high development of firing phases including gehlenite, diopside, and plagioclase, which pointed to an EFT in the range 850–950 °C, probably over 900 °C. Illite-muscovite was present, but always with low intensity. The amphorae from SR showed a beige-yellow color to the naked eye; only in rare cases (BET-9 and BET-27), there was a more pinkish-orange color in the walls of the ceramic section, with a beige-yellow core. The low variation in the XRD spectra for SR samples indicated a higher homogeneity in the firing temperatures of the amphorae from this kiln site and, possibly, a better control of firing conditions compared with the other three workshops analyzed.

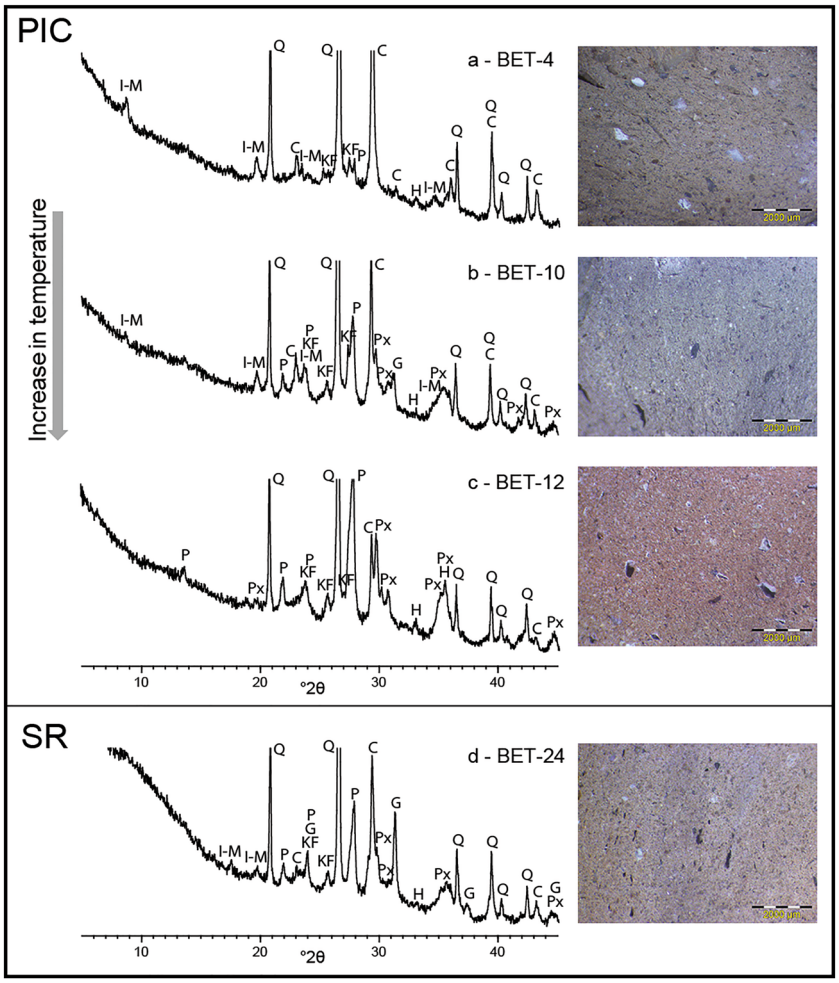

Fig. 6 XRD spectra for selected samples from PIC (a–c) and SR (d), and photographs of each individual taken at × 15. Abbreviations for minerals: Q quartz, P plagioclase, KF alkali feldspar, C calcite, G gehlenite, Px pyroxene, H hematite, I-M illite-muscovite

Chemical analysis (XRF)

The normalized chemical results (Table 2) showed a relatively homogeneous composition for all the amphorae analyzed, except for variations in a series of elements. The main variability was apparently related to some major and minor elements, in particular CaO, Al_2O_3, P_2O_5, MgO, and Na_2O. All the individuals were calcareous, with CaO percentages ranging between 8.7 and 20.1%, while Al_2O_3 percentages varied between 12.3 and 16.9%. The samples from Azanaque-Castillejo (AZ) usually showed lower CaO and higher Al_2O_3 than the others, whereas an inverse trend was observed for the amphorae from Las Monjas-Soto del Rey (SR); instead, the samples from Isla de la Barqueta (IB) and Picachos (PIC) usually presented intermediate values for both elements. Samples from AZ were also characterized by a lower MgO content than the amphorae from IB, SR, and PIC. A CaO vs MgO bivariate plot (Fig. 7a) clearly showed the differentiation of AZ from the other workshops, while SR formed a separate group as well, due to its higher CaO percentages. This differentiation of AZ was consistent with the petrographic results, which showed a lower calcareous composition of the matrix and inclusions in the samples from this workshop compared to those of IB, SR, and PIC (except for sample BET-19 from IB).

The content in Na_2O was usually slightly lower in SR and higher in IB, but with exceptions. Conversely, variations in P_2O_5 did not show any relation to clear differences among workshops (Table 2).

With regard to trace element composition, the data (Table 2) suggested a general similarity between the four kiln sites analyzed except for differences in a few elements, mainly V, Zn, and Cr. The concentrations of these three elements tended to be higher in the samples from AZ, while V and Cr were usually lower in SR samples than in the others. These differences were clearly observed in the V vs Cr bivariate plot (Fig. 7b). There was also certain variability in the content of Ba in the data set, which tended to be relatively low in AZ; however with many exceptions, that did not enable using this element as a geochemical marker for differentiating among the workshops under study.

The calculation of the Compositional Variation Matrix or CVM (Aitchison 1986, 2005; Buxeda 1999; Buxeda and Kilikoglou 2003) provided more details on the chemical variability of the data set. The total variation (*vt*) value, 0.46, was

Table 2 Chemical composition of the amphora samples analyzed through XRF, normalized on an anhydrous basis. Concentrations of major and minor oxides are in percent; other minor and trace elements are in parts per million. For each kiln site, mean (m) and standard deviation (sd) values are given (in italics)

Sample	Fe_2O_3	Al_2O_3	MnO	P_2O_5	TiO_2	MgO	CaO	Na_2O	K_2O	SiO_2	Ba	Rb	Th	Nb	Pb	Zr	Y	Sr	Ce	Ga	V	Zn	Cu	Ni	Cr
Azanaque-Castillejo (AZ)																									
BET-1	6.75	16.32	0.05	0.32	0.86	2.37	11.14	0.59	2.62	58.82	345	100	12	17	17	182	24	305	74	20	164	98	18	39	120
BET-2	6.30	15.54	0.05	0.59	0.81	2.17	12.53	0.57	2.36	58.91	399	95	12	16	18	192	23	295	71	20	144	96	17	38	127
BET-3	6.90	16.76	0.05	0.43	0.86	2.34	11.40	0.60	2.56	57.93	353	106	14	18	17	188	25	327	80	21	168	106	21	40	139
BET-33	6.67	16.12	0.05	0.25	0.85	2.39	12.14	0.58	2.28	58.52	324	95	13	17	16	170	23	279	76	19	158	99	18	39	126
BET-34	6.94	16.76	0.05	0.29	0.87	2.52	10.72	0.69	2.45	58.56	357	104	12	18	15	186	25	313	78	21	177	104	19	41	137
BET-35	6.70	16.79	0.05	0.30	0.87	2.45	11.34	0.57	2.46	58.30	356	102	13	18	17	181	24	314	75	20	162	101	18	42	134
BET-36	6.74	16.56	0.05	0.33	0.86	2.03	10.47	0.45	2.47	59.87	550	93	12	17	17	178	24	297	75	20	165	99	18	40	115
m	*6.71*	*16.41*	*0.05*	*0.36*	*0.86*	*2.32*	*11.39*	*0.58*	*2.46*	*58.70*	*383*	*99*	*13*	*17*	*17*	*183*	*24*	*304*	*76*	*20*	*163*	*100*	*18*	*40*	*128*
sd	*0.21*	*0.46*	*0.00*	*0.12*	*0.02*	*0.17*	*0.73*	*0.07*	*0.11*	*0.61*	*77*	*5*	*1*	*1*	*1*	*7*	*1*	*16*	*3*	*1*	*10*	*4*	*1*	*1*	*9*
Picachos (PIC)																									
BET-4	5.30	13.15	0.06	0.19	0.70	2.97	16.17	0.49	2.61	58.22	390	90	12	14	22	184	22	326	65	16	124	79	16	31	87
BET-5	5.99	15.21	0.05	0.22	0.80	2.75	13.97	0.59	2.39	57.87	479	88	13	16	20	193	24	285	79	19	147	90	17	35	113
BET-10	5.99	14.84	0.06	0.22	0.78	3.48	15.31	0.44	2.62	56.12	358	91	13	16	16	186	24	317	80	19	133	88	19	35	112
BET-11	6.00	14.73	0.06	0.22	0.76	3.32	13.90	0.46	2.57	57.82	536	90	12	15	19	180	23	272	68	18	134	88	19	34	100
BET-12	6.62	16.49	0.07	0.22	0.84	3.25	12.75	0.56	2.46	56.58	534	78	13	17	17	185	25	339	81	20	141	92	19	44	124
BET-13	6.38	15.67	0.06	0.30	0.82	3.31	12.62	0.58	2.78	57.33	374	105	13	17	15	187	25	351	74	19	158	94	18	35	120
m	*6.05*	*15.02*	*0.06*	*0.23*	*0.78*	*3.18*	*14.12*	*0.52*	*2.57*	*57.32*	*445*	*90*	*13*	*16*	*18*	*186*	*24*	*315*	*75*	*18*	*140*	*88*	*18*	*36*	*109*
sd	*0.45*	*1.12*	*0.00*	*0.04*	*0.05*	*0.27*	*1.40*	*0.07*	*0.14*	*0.82*	*81*	*9*	*0*	*1*	*3*	*4*	*1*	*31*	*7*	*1*	*12*	*5*	*1*	*4*	*14*
Isla de la Barqueta (IB)																									
BET-6	5.86	14.58	0.05	0.22	0.77	3.13	15.44	0.81	2.22	56.77	399	81	13	16	16	189	24	371	68	18	128	87	16	34	103
BET-7	6.07	15.36	0.05	0.60	0.80	3.12	14.07	0.83	2.45	56.47	403	97	13	16	15	270	25	421	76	17	129	86	16	37	115
BET-16	5.85	14.37	0.05	0.24	0.77	2.77	16.48	0.78	2.37	56.17	381	92	13	15	16	194	24	364	67	18	132	87	16	32	107
BET-17	6.08	14.96	0.05	0.24	0.78	2.95	15.68	0.80	2.54	55.76	407	98	13	16	16	180	24	398	72	19	124	90	16	36	106
BET-18	6.45	15.42	0.05	0.23	0.81	2.91	13.37	0.70	2.55	57.34	411	98	12	16	17	190	25	334	76	17	121	90	16	38	114
BET-19	6.74	16.89	0.05	0.29	0.88	2.82	8.67	0.73	2.84	59.92	577	103	13	17	18	185	25	295	77	20	158	97	17	39	121
BET-20	5.63	14.01	0.08	0.23	0.72	3.40	17.67	0.51	2.26	55.31	598	76	11	15	15	170	23	386	66	17	131	87	19	35	105
BET-21	6.17	15.36	0.05	0.34	0.81	2.81	14.00	0.63	2.47	57.18	557	89	13	16	18	192	25	380	76	18	142	91	17	37	111
BET-22	6.03	14.55	0.05	0.24	0.79	2.85	13.87	0.59	2.31	58.57	410	81	12	15	15	193	24	307	72	17	132	88	15	35	115
m	*6.10*	*15.05*	*0.06*	*0.29*	*0.79*	*2.97*	*14.36*	*0.71*	*2.45*	*57.05*	*460*	*91*	*13*	*16*	*16*	*196*	*24*	*362*	*72*	*18*	*133*	*89*	*17*	*36*	*111*
sd	*0.33*	*0.85*	*0.01*	*0.12*	*0.04*	*0.21*	*2.56*	*0.11*	*0.19*	*1.44*	*89*	*9*	*1*	*1*	*1*	*29*	*1*	*42*	*4*	*1*	*11*	*3*	*1*	*2*	*6*
Soto del Rey-Las Monjas (SR)																									
BET-8	5.38	13.45	0.07	0.62	0.72	3.50	17.58	0.40	2.55	55.55	631	74	12	14	17	185	24	349	71	16	98	81	21	35	76
BET-9	5.41	13.93	0.07	0.32	0.73	3.37	18.23	0.46	2.68	54.64	444	92	13	14	16	176	24	358	74	17	110	83	21	35	89
BET-24	5.49	13.81	0.07	0.41	0.72	3.25	18.50	0.39	2.61	54.57	485	96	12	15	18	182	25	368	70	17	126	88	24	36	94
BET-25	5.29	13.51	0.07	0.41	0.71	3.14	18.64	0.40	2.63	55.03	462	95	12	15	16	188	24	371	63	17	120	83	22	35	92
BET-26	5.42	13.74	0.07	0.44	0.73	3.16	17.29	0.42	2.68	55.89	501	95	12	15	16	188	24	358	63	17	118	84	21	35	94
BET-27	5.34	13.53	0.07	0.34	0.72	3.33	18.38	0.42	2.60	55.10	511	95	13	15	17	193	25	382	67	16	105	87	23	37	90
BET-28	4.83	12.28	0.08	0.31	0.67	3.61	20.08	0.40	2.56	55.02	555	84	11	13	18	193	23	359	56	15	95	77	23	31	82
BET-29	5.16	12.72	0.08	0.40	0.70	3.47	19.01	0.42	2.68	55.21	529	89	12	14	11	197	25	396	66	15	101	91	23	34	81
m	*5.29*	*13.37*	*0.07*	*0.41*	*0.71*	*3.35*	*18.46*	*0.41*	*2.62*	*55.13*	*515*	*90*	*12*	*15*	*16*	*187*	*24*	*368*	*66*	*16*	*109*	*84*	*22*	*35*	*87*
sd	*0.21*	*0.57*	*0.01*	*0.10*	*0.02*	*0.17*	*0.86*	*0.02*	*0.05*	*0.44*	*59*	*8*	*0*	*1*	*2*	*7*	*1*	*15*	*6*	*1*	*11*	*4*	*1*	*2*	*7*

relatively low, and even lower (0.34) after excluding two elements (P_2O_5 and Pb) usually related to problems of alteration/contamination in ceramics. Such low values might be possibly associated with a monogenic population (Buxeda and Kilikoglou 2003). In fact, the CVM showed that no element presented a very high $\tau_{.i}$ (variance) value. The elements that introduced more variability in the data set were P_2O_5 ($\tau_{.i}$ = 2.87), CaO ($\tau_{.i}$ = 1.78) and Na_2O ($\tau_{.i}$ = 1.78), followed by Ba, MnO, MgO, V, and Cr. Much of this variation could be associated with geochemical differences between workshops, in particular with regard to CaO, Na_2O, MgO, V, and Cr, as suggested by Table 2.

A cluster analysis of the chemical data allowed for a better examination of this variability; the concentrations were previously transformed into additive log-ratios (alr) using Y as a divisor, since it was the element with the lowest variance ($\tau_{.i}$) according to the CVM. Three main clusters could be differentiated in the dendrogram (Fig. 8): cluster A, which included samples from SR; cluster B, with samples from IB and PIC; and cluster C, which corresponded to samples from AZ. The clear distinction of SR and AZ, each as separate clusters, must be associated with the already mentioned particularities in major, minor, and trace elements for the chemical reference groups from these workshops (Table 2; Fig. 7). These differences between kiln sites were also observed through a principal component analysis (PCA) (Fig. 9), in which PC1, accounting for 61% of the total variance, was dominated by negative loadings of CaO and MgO and positive of Na_2O, V, and Cr, while negative loadings of Na_2O were dominating PC2, which explains 15% of the variance. Consequently, in the PC1 vs PC2 biplot, the samples from SR, with relatively high content in CaO and MgO, and low in Na_2O, V and Cr, showed negative scores of PC1, while the group from AZ presented positive PC1 scores due to its low content in CaO and MgO and high in V and Cr (Figs. 7 and 9).

As for the samples from IB and PIC, the multivariate statistical treatment (Figs. 8 and 9) and the examination of the chemical data (Table 2) did not provide evidence of significant compositional differences among the amphorae from both sites. Na_2O was usually slightly higher in IB than in PIC, as also observed in the PCA (Fig. 9), but a clear differentiation between both workshops cannot be established on this basis only. Therefore, it must be accepted that a certain chemical overlap may exist between the reference groups from IB and PIC (Table 2).

The presence of one sample from IB, BET-19, behaving as a chemical loner (Figs. 8 and 9) might suggest the existence of a higher chemical variability for this kiln site, but other possible interpretations for this loner could not be excluded (e.g., more than one production at the same workshop? an amphora not produced in this site but imported?). This sample (BET-19) differed from the other IB amphorae in its lower content in CaO (8.7%) and higher in Fe_2O_3 and Al_2O_3 (Table 2; Fig. 7a). This was consistent with the results of petrographic and mineralogical analyses, since a lower abundance of carbonate inclusions was observed in this individual in thin section, and lower peaks of calcite were found in its XRD spectra.

A comparison with reference groups for Early Roman kiln sites in the study area

The four Late Roman workshops analyzed in this work were compared to existing chemical reference groups from Early Roman amphora kiln sites in the Guadalquivir valley. Only for

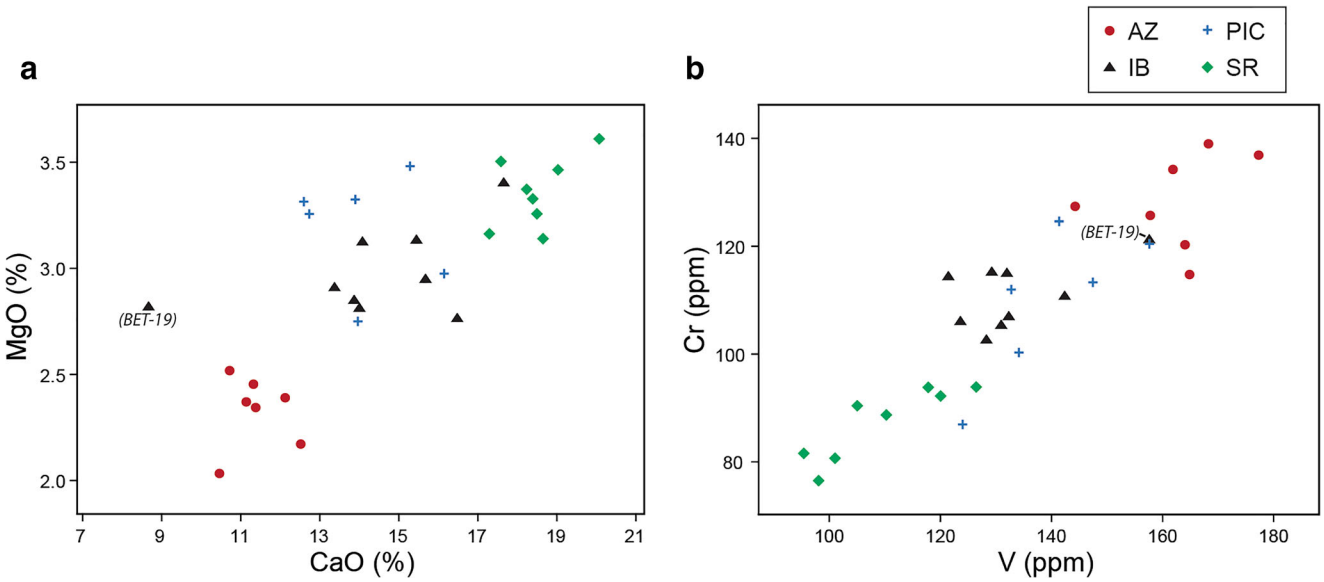

Fig. 7 Binary diagrams, using normalized data, of **a** CaO vs MgO and **b** V vs Cr for the amphora samples analyzed. An indication of the kiln site for each individual is given

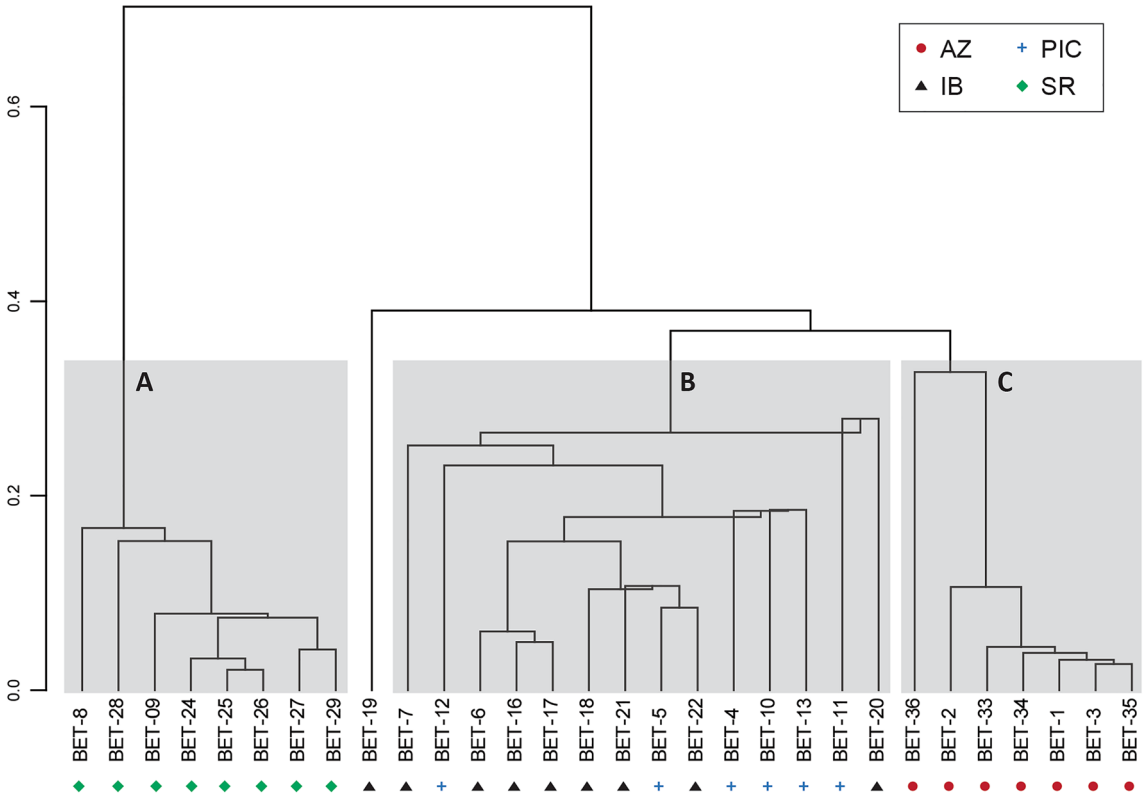

Fig. 8 Cluster analysis, using the centroid agglomerative method and the squared Euclidean distance, based on the alr transformed subcomposition Fe_2O_3, Al_2O_3, TiO_2, MgO, CaO, Na_2O, K_2O, SiO_2, Ba, Rb, Th, Nb, Zr, Sr, Ce, Ga, V, Zn, Cu, Ni, and Cr (Y was used as divisor). An indication of the kiln site for each individual is given

two Early Roman kiln sites, El Tejarillo (TJ) and La Catria (CTR) (Fig. 2), compositional groups based on major, minor and chemical trace elements—determined through XRF—have been published so far (Grubessi and Conti 1999) (Table 3). Such analysis was also carried out on an Early Roman kiln site in Sevilla (Polvorinos del Río et al. 2003), albeit only very few of the analyzed samples resulted to be locally produced actually. For a few other workshops that were chemically characterized (Grubessi 1999; González Vílchez et al. 2001), the lack of data on trace element composition made the comparison more difficult.

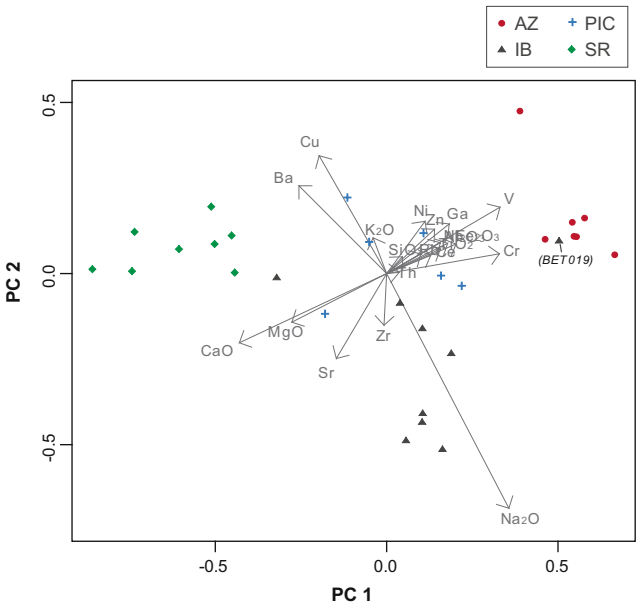

Fig. 9 PCA based on the same alr transformed subcomposition as the cluster analysis. Plot of principal components 1 and 2 (PC1 vs PC2) with their scores and loadings. PC1 and PC2 account for 61% and 15% of the total variance, respectively. An indication of the kiln site for each individual is given

Both TJ and, apparently, CTR continued to produce amphorae in the Late Roman period (Remesal 1983, 1991; cf. Bourgeon 2017); however, the published chemical data was based on Early Roman Dressel 20 amphorae, so they should not be taken as reliable reference groups for Dressel 23 from the same sites, since there is no evidence of continuity in the use of the same sources of raw materials during the Late Roman period. In any case, comparison between normalized chemical data from these Early Roman kiln sites (Table 3) and the data from Late Roman production sites analyzed in the present research (Table 2) showed some compositional differences between them. The amphorae from both TJ and CTR were characterized by higher SiO_2% as well as a lower content in Ba and Zr than the samples from the other four workshops; the lowest Zr concentrations were found in CTR, while Ba tended to be lower in TJ (Table 3). In addition, MgO and CaO

Table 3 Chemical data (XRF) of the Early Roman amphora kiln sites analyzed by Grubessi and Conti (1999); compositions are normalized on an anhydrous basis. Concentrations of major and minor oxides are in percent; other minor and trace elements are in parts per million. For each kiln site, mean (m) and standard deviation (sd) values are given (in italics)

Sample	Fe_2O_3	Al_2O_3	MnO	P_2O_5	TiO_2	MgO	CaO	Na_2O	K_2O	SiO_2	Ba	Rb	Th	Nb	Pb	Zr	Y	Sr	Ce	Ga	V	Zn	Cu	Ni
La Catria (CTR)																								
CTR 1	5.85	15.11	0.05	0.22	0.78	2.30	12.97	0.38	2.48	59.74	311	88	9	17	19	146	20	293	62	19	121	82	15	33
CTR 10/1	5.76	15.09	0.05	0.26	0.77	1.73	11.45	0.32	2.41	62.04	466	73	6	15	19	140	18	231	53	16	100	74	15	31
CTR 10/2	5.89	15.24	0.05	0.25	0.78	2.06	12.32	0.45	2.26	60.58	370	85	8	17	22	151	21	288	59	19	119	84	15	35
CTR 10/3	5.67	14.69	0.05	0.30	0.77	2.18	12.07	0.42	2.54	61.19	280	84	8	16	23	141	20	304	55	18	116	80	15	31
CTR 24/1	5.88	15.29	0.05	0.30	0.79	2.38	11.99	0.43	2.44	60.33	309	87	8	16	22	144	20	291	51	18	119	81	14	32
CTR 24/5	5.54	14.23	0.05	0.35	0.72	2.05	11.25	0.55	2.45	62.68	374	90	8	15	20	136	19	295	55	18	101	77	15	32
CTR 24/6	5.95	15.57	0.05	0.39	0.78	2.28	12.28	0.44	2.53	59.59	339	94	10	18	24	151	20	323	59	19	125	84	17	33
CTR 24/8	5.83	15.06	0.05	0.39	0.78	2.03	11.56	0.42	2.24	61.52	326	84	8	17	20	145	19	279	57	18	112	81	16	32
CTR 24/9	5.25	15.84	0.05	0.30	0.74	2.35	11.70	0.49	2.49	60.66	265	79	8	16	19	145	20	273	55	18	119	82	15	33
CTR 4/12	6.26	15.54	0.05	0.44	0.82	2.20	11.75	0.50	2.54	59.78	294	91	9	17	20	150	20	296	58	18	110	81	17	32
CTR 4/13	5.82	15.08	0.05	0.29	0.76	2.14	12.23	0.49	2.39	60.62	293	94	8	16	20	153	21	313	55	19	111	83	15	34
CTR 4/14	5.98	15.10	0.05	0.27	0.73	2.69	12.74	0.40	2.49	59.43	337	86	8	16	17	144	19	275	52	18	112	81	15	33
CTR 4/6	5.31	18.24	0.04	0.27	0.67	1.82	10.56	0.40	2.57	60.00	277	81	8	15	21	138	19	278	51	17	117	79	14	32
CTR 4/7	5.83	14.91	0.05	0.28	0.76	2.16	11.86	0.46	2.45	61.14	213	82	7	15	22	136	19	266	43	17	114	79	14	31
CTR 4/9	5.76	14.68	0.05	0.28	0.73	2.41	13.52	0.42	2.51	59.53	280	94	8	17	19	149	21	336	53	18	110	86	16	33
m	*5.77*	*15.31*	*0.05*	*0.31*	*0.76*	*2.19*	*12.02*	*0.44*	*2.45*	*60.59*	*316*	*86*	*8*	*16*	*20*	*145*	*20*	*289*	*55*	*18*	*114*	*81*	*15*	*32*
sd	*0.25*	*0.90*	*0.00*	*0.06*	*0.04*	*0.24*	*0.72*	*0.06*	*0.10*	*0.97*	*59*	*6*	*1*	*1*	*2*	*6*	*1*	*25*	*5*	*1*	*7*	*3*	*1*	*1*
El Tejarillo (TJ)																								
TJ 81/101	5.76	14.27	0.05	0.29	0.75	2.56	11.60	0.53	2.40	61.69	241	75	7	16	21	164	20	279	59	17	106	79	13	30
TJ 81/211	5.75	14.09	0.05	0.25	0.71	2.36	12.33	0.62	2.47	61.24	241	85	9	16	27	165	21	284	51	17	106	79	13	31
TJ 81/215	5.68	14.15	0.05	0.27	0.74	2.41	11.17	0.57	2.44	62.40	237	85	8	16	21	156	19	291	47	17	111	77	13	30
TJ 81/216	6.06	14.64	0.05	0.28	0.78	2.40	10.75	0.67	2.60	61.66	263	89	9	18	16	171	20	300	60	18	119	87	15	33
TJ 81/55	5.81	14.36	0.04	0.28	0.72	2.04	10.89	0.55	2.35	62.84	239	86	8	15	17	156	19	283	52	17	114	79	12	30
TJ 81/56	5.87	14.02	0.04	0.28	0.75	2.39	12.68	0.60	2.39	60.88	223	82	6	15	17	153	19	305	52	17	105	79	14	30
TJ 81/688	5.94	14.61	0.05	0.32	0.76	2.44	12.10	0.53	2.39	60.74	262	88	9	17	19	174	22	284	62	18	107	82	14	33
TJ 81/73	5.75	14.06	0.05	0.31	0.72	2.29	12.02	0.53	2.27	61.88	257	86	8	16	18	162	20	296	55	17	115	78	13	30
TJ 81/74	5.96	14.69	0.04	0.28	0.78	2.25	10.50	0.50	2.34	62.54	248	84	8	16	17	169	20	282	57	17	119	79	12	31
TJ 81/76	5.85	14.50	0.05	0.27	0.76	3.16	9.71	0.51	2.22	62.85	232	82	7	17	19	160	20	281	56	18	114	82	13	32
TJ 81/85	6.16	14.96	0.05	0.30	0.74	3.28	11.01	0.50	2.28	60.59	278	88	9	17	19	177	21	306	59	18	122	89	14	33
TJ 81/89	5.94	14.73	0.05	0.27	0.76	2.42	11.33	0.59	2.46	61.32	265	89	7	17	19	173	21	323	60	17	114	87	14	33
TJ 81/93	5.68	14.21	0.04	0.28	0.77	2.18	11.67	0.60	2.34	62.11	248	85	9	16	20	164	20	288	50	16	103	77	13	31
m	*5.86*	*14.41*	*0.05*	*0.28*	*0.75*	*2.48*	*11.37*	*0.56*	*2.38*	*61.75*	*249*	*85*	*8*	*16*	*19*	*165*	*20*	*293*	*55*	*17*	*112*	*81*	*13*	*31*
sd	*0.15*	*0.30*	*0.00*	*0.02*	*0.02*	*0.36*	*0.82*	*0.05*	*0.10*	*0.77*	*15*	*4*	*1*	*1*	*3*	*8*	*1*	*13*	*5*	*1*	*6*	*4*	*1*	*1*

percentages in samples from TJ and CTR were similar to those from AZ and lower than in IB, PIC and SR. These differences in major elements and traces were better observed in the bivariate plots MgO vs Ba (Fig. 10a) and SiO_2 vs Zr (Fig. 10b). Also the multivariate statistical analysis of the chemical data provided a tool for their differentiation, as shown by a PCA based on the alr transformed chemical subcomposition Fe_2O_3, Al_2O_3, TiO_2, MgO, CaO, Na_2O, K_2O, SiO_2, Ba, Rb, Th, Nb, Zr, Sr, Ce, Ga, V, Zn, Cu, and Ni, using Y as a divisor (Fig. 11). In this case, PC1 was dominated by negative loadings of Ba and CaO and positive of Na_2O, Nb, and SiO_2, while PC2 was dominated by positive loadings of Na_2O. The aforementioned particularities of TJ and CTR concerning the content in CaO, SiO_2, MgO, and Ba were clearly affecting the PC1 and PC2 scores of their individuals in the PCA; the loadings of Na_2O in the PCA were related to slightly higher concentrations of this element in IB and lower in SR and CTR (Tables 2 and 3). The analysis suggested that the samples from TJ and CTR were more similar in composition to amphorae from AZ than to those from the other three sites (Fig. 11); this is significant since these workshops (TJ, CTR, and AZ) are located relatively close to each other (Fig. 2) and were probably using similar source/s of raw materials. It is worth mentioning that Cr was not determined for the amphorae from TJ and CTR (Grubessi and Conti 1999); this might be a constraint for comparison, since Cr proved to be an useful marker for the differentiation between some of the Late Roman workshops analyzed (Fig. 7b).

In summary, comparison between the chemical reference groups from Dressel 23 kiln sites and those from Dressel 20 workshops published by Grubessi and Conti (1999) suggested the existence of compositional differences between them. These variations may be related to the use of slightly different raw materials and/or paste recipes, possibly due to the specific location of each site along the Guadalquivir valley, but not excluding also possible technological differences between Early Roman and Late Roman amphora production that could account for this compositional variability. Nevertheless, it also could not be excluded that the chemical differences between the samples from TJ and CTR and those from the Late Roman workshops analyzed in this work were associated with the different instruments and calibration standards used for the XRF analysis in each case. For this reason, the comparison between these data sets should be taken with caution.

Summary and conclusions

The scientific analysis of Dressel 23 amphorae from four kiln sites in the Guadalquivir valley and its main tributary, the Genil valley, showed the presence of rather similar fabrics but still with slight petrographic and/or chemical variations between them, which were useful for their differentiation. The amphorae from these four sites were produced using calcareous clayey raw materials, with strong similarities in terms of petrographic and mineralogical composition and textural parameters. This suggested that the potters from the four workshops were following, in general terms, approximately similar technological choices and procedures, with minor differences. The amphorae from AZ showed a slightly more distinct chemical-petrographic composition, also characterized by the use

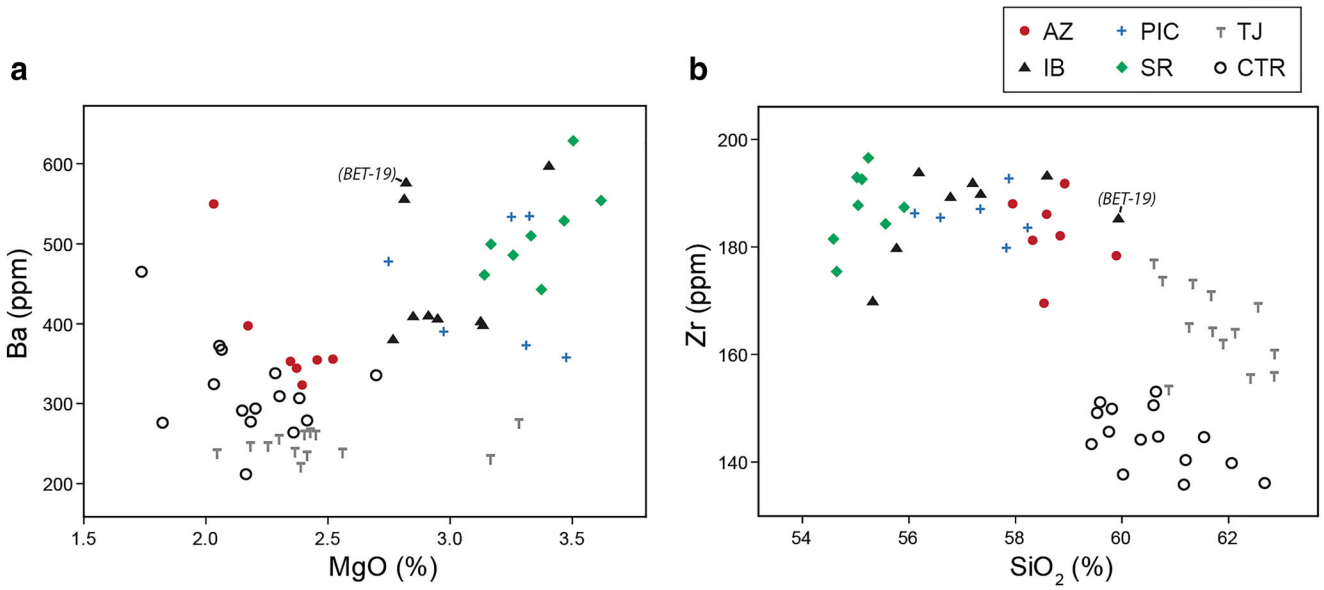

Fig. 10 Binary diagrams, using normalized data, of **a** MgO vs Ba and **b** SiO_2 vs Zr for the four Late Roman kiln sites analyzed in this work (AZ, IB, PIC, and SR) and two Early Roman kiln sites analyzed by Grubessi and Conti (1999) (CTR and TJ). Sample BET-7 (IB), with very high Zr, was not included in **b** in order to better visualize the patterns

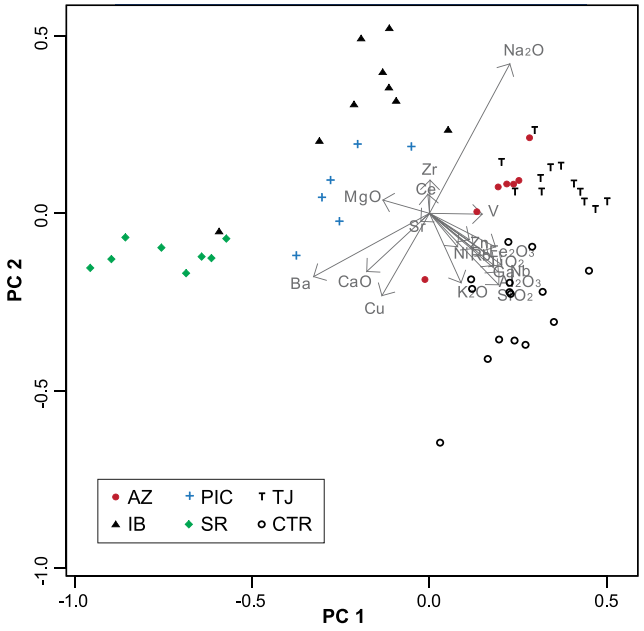

Fig. 11 PCA comparing the composition of amphorae from the Late Roman kiln sites analyzed in this work (AZ, IB, PIC, and SR) and the Early Roman kiln sites analyzed by Grubessi and Conti (1999) (CTR and TJ). The analysis is based on the same alr transformed chemical subcomposition as in Fig. 9 but excluding Cr (no data for Cr was provided by Grubessi and Conti 1999); Y was used as divisor. PC1 and PC2 account for 49% and 17% of the total variance, respectively

of carbonate-rich clayey sediments but still less calcareous than the amphorae from the other three sites analyzed (IB, PIC and SR); this characteristic accounted for the more reddish color observed in AZ samples macroscopically. This higher differentiation of AZ might be related to the fact that this site is located farther downriver than the other three kiln sites, while these latter are geographically closer to each other (Fig. 2). In fact, the amphorae from IB, PIC, and SR proved to be indistinguishable from each other in terms of petrographic fabrics; however, the XRF analysis indicated that a number of major and trace elements (in particular, CaO, Al_2O_3, V, and Cr) may be used as geochemical markers for differentiating the amphorae produced in SR from those coming from IB and PIC. As for these latter, no significant petrographic, mineralogical, or chemical differences were found between the amphorae from both sites. The existence of a geochemical overlap between the reference groups of IB and PIC might be indicating that a highly similar source of raw materials and similar paste recipes was used in both workshops, while in SR, a nearby source was probably used, also similar to the one used in IB and PIC but with slight compositional differences.

The kiln sites analyzed in this study are located on terrains dominated by Quaternary alluvial deposits with contribution of materials from various sources, including abundant marls and other calcareous sedimentary deposits, especially from the Tertiary, as well as metamorphic and igneous materials from the Sierra Morena. Calcareous clays, exploited as raw material by modern ceramic and brick factories, have been reported in several areas throughout this region, including areas close to the sites under study and to other ancient pottery kiln sites (e.g., González García and García Ramos 1964, 1965; García Ramos et al. 1966; IGME 1980). As for the four kiln sites analyzed, the occurrence of similar fabrics but with slight compositional variations, in some cases indistinguishable through thin section petrography, would indicate the procurement of approximately similar clays—related to the same geological formation—but from different locations within the Guadalquivir and Genil basin, most likely from the vicinity of the sites. Since potential clayey sources for ceramic production were widely available throughout the region, it is highly plausible the hypothesis that these raw materials were collected locally. The nature and textural characteristics of the inclusions observed in the petrographic fabrics suggest that the Quaternary alluvial deposits surrounding the production sites could have been likely sources of clays; unfortunately, it was not possible in this study to sample potential sources of raw clays in the field in order to verify this hypothesis.

Exploitation of slightly distinct clay sources could account for part of the variability observed in the petrographic analysis, particularly in the case of AZ compared to IB, PIC, and SR. Besides raw material selection, another part of this variability could be associated with technological variations related to other phases of the *chaîne opératoire*, such as raw material processing, paste preparation and firing (Lemonnier 1976; Sillar and Tite 2000; Quinn 2013). In the absence of geological clay samples for comparison, it was not possible to ascertain whether the fine-medium sandy inclusions observed in the fabrics were the result of intentionally added temper or naturally occurring inclusions of the clay source, although the latter seems more plausible based on the petrographic evidence. The gradual textural variability observed in the fabrics, even within the same workshop, may be the result not only of natural variations of the exploited clay deposits but also of differences in the refining of clays (i.e., through sieving or levigation) during raw material processing. In any case, the results pointed to the use of very similar paste recipes in the four kiln sites analyzed.

Further variations were identified concerning the firing process. In general, the amphorae manufactured in these workshops were usually fired at temperatures of ca. 850–950 °C and under reducing-oxidizing atmospheres. However, while the samples from SR showed relatively consistent firing conditions, higher variability in both firing temperatures and atmosphere was found in samples from IB, PIC, and, to a lesser degree, AZ. These variations

within the same kiln site can be common in closed firings, even in a single pot (Quinn 2013). Nevertheless, the observed differences in the uniformity of firing characteristics among kiln sites may suggest the occurrence of differences in potters' choices and/or control over the firing process.

In summary, the slight compositional and fabric variability identified in the amphora assemblage may be associated with both natural variation of raw materials and technological aspects, with differences between not only kiln sites but also some internal variabilities within the same site. Nevertheless, despite this minor variability, the general results indicated strong parallels in terms of technological choices and procedures between the four workshops analyzed, resulting in quite similar fabrics which are hardly distinguishable from each other to the naked eye and even under thin section. Moreover, the forms of amphorae produced in these sites, mostly related to type Dressel 23a, were quite homogeneous (Bourgeon 2017), although with slight morphological variations that seem to be partially associated with differences between workshops (Berni and Moros 2012). The function of these ceramics should also be considered in the interpretation of technological choices made by the potters (Lemonnier 1993; Schiffer and Skibo 1997; Sillar and Tite 2000), since amphorae were not a consumption good by themselves but, instead, transport containers for trading foodstuffs (oil in this case). For this reason, a high level of technological standardization is not necessarily expected in their production, as could be inferred from the intra- and inter-variability found in the kiln sites producing Dressel 23a. In any case, the documentation of some standardized patterns, in aspects such as paste recipes and the general form and size of the amphorae, should be understood in the context of industrial mass production of amphorae for exporting oil throughout the Guadalquivir and Genil valleys in the Late Roman period (Remesal 2004; Berni and Moros 2012).

The present research provided, for the first time, a scientific characterization of Late Roman amphorae of type Dressel 23 from kiln sites in this region, therefore shedding new light on their compositional and technological characteristics. Furthermore, the results obtained enabled the definition of at least three differentiated reference groups (AZ, SR, and IB-PIC) for kiln sites producing these amphorae, which will be useful for their identification in consumption sites through provenance studies. This is a first step towards the construction of an archaeometric reference database for Late Roman kiln sites in the Guadalquivir valley, which will certainly help to better investigate the production and export of oil transported in Dressel 23 amphorae, as well as to examine in more detail the trade connections between the various production sites in this region and consumption sites across the Mediterranean.

Acknowledgments This work was performed in the framework of the project *Late Roman Pottery in the Western Mediterranean: exploring regional and global trade networks through experimental sciences (LRPWESTMED)* (ref. HAR2013-45874-P), funded by the National Plan of I + D + I Ministerio de Economía y Competitividad, Secretaría de Estado de Investigación, Desarrollo e Innovación, with contributions from FEDER funds, PI: Miguel Ángel Cau Ontiveros. This is part of the activities of the Equip de Recerca Arqueològica i Arqueomètrica de la Universitat de Barcelona (ERAAUB), Consolidated Group (2017 SGR 1043), thanks to the support of the Comissionat per a Universitats I Recerca del DIUE de la Generalitat de Catalunya. Research by L. Fantuzzi was carried out in the framework of a postdoctoral fellowship Juan de la Cierva-Formación, supported by the Spanish Ministerio de Ciencia, Innovación y Universidades. We are indebted to Piero Berni Millet (Institut Català d'Arqueologia Clàssica) and Juan Moros Díaz (CEIPAC, Universitat de Barcelona) for providing the samples from the kiln sites analyzed in this work. XRF and XRD analyses were undertaken at the Centres Científics i Tecnològics of the University of Barcelona.

References

Aitchison J (1986) The statistical analysis of compositional data. Chapman and Hall, London

Aitchison J (2005) A concise guide to compositional data analysis. In: 2nd Compositional Data Analysis Workshop (CoDaWork'05). Universitat de Girona, Girona. http://ima.udg.edu/Activitats/CoDaWork05/A_concise_guide_to_compositional_data_analysis.pdf.

Baldomero A, Corrales P, Escalante MM, Serrano E, Suárez J (1997) El alfar romano de la Huerta del Rincón: síntesis tipológica y momentos de producción. In: Figlinae Malacitanae: la producción de cerámica romana en los territorios malacitanos. Área de Arqueología de la Universidad de Málaga, Málaga, pp 147–176

Beltrán M (1970) Las ánforas romanas en España. Institución Fernando el Católico, Zaragoza

Bernal D (1997) Las producciones ánforicas del Bajo Imperio y de la Antigüedad Tardía en Málaga. Estado actual de la investigación e hipótesis de trabajo. In: Figlinae Malacitanae: la producción de cerámica romana en los territorios malacitanos. Área de Arqueología de la Universidad de Málaga, Málaga, pp 233–260

Bernal D (2001) La producción de ánforas en la Bética en el s. III y durante el bajo imperio romano. In: Congreso Internacional Ex Baetica Amphorae. Conservas, aceite y vino de la Bética en el Imperio Romano (Écija, Sevilla, 1998). Gráficas Sol, Écija, pp 239–372

Berni P (1998) Las ánforas de aceite de la Bética y su presencia en la Cataluña romana. Publicacions Universitat de Barcelona, Barcelona

Berni P (2008) Epigrafía anfórica de la Bética: nuevas formas de análisis. Publicacions Universitat de Barcelona, Barcelona

Berni P, García Vargas E (2016) Dressel 20 (Valle del Guadalquivir). In: Amphorae ex Hispania. Paisajes de producción y de consumo. Institut Català d'Arqueologia Clàssica. http://amphorae.icac.cat/amphora/dressel-20-guadalquivir-valley. Accessed 10 June 2019

Berni P, Moros J (2012) Los sellos in planta pedis de las ánforas olearias béticas Dressel 23 (primera mitad siglo V d.C.). Arch Esp Arqueol 85:193–219

Berni P, Moros J (2017) Dressel 23 (Valle del Guadalquivir). In: Amphorae ex Hispania. Paisajes de producción y de consumo. Institut Català d'Arqueologia Clàssica. http://amphorae.icac.cat/amphora/dressel-23-guadalquivir-valley. Accessed 10 June 2019

Blázquez JM, Remesal J (1999) Estudios sobre el Monte Testaccio (Roma) I. Publicacions Universitat de Barcelona, Barcelona

Blázquez JM, Remesal J (2001) Estudios sobre el Monte Testaccio (Roma) II. Publicacions Universitat de Barcelona, Barcelona

Blázquez JM, Remesal J (2003) Estudios sobre el Monte Testaccio (Roma) III. Publicacions Universitat de Barcelona, Barcelona
Blázquez JM, Remesal J (2007) Estudios sobre el Monte Testaccio (Roma) IV. Publicacions Universitat de Barcelona, Barcelona
Blázquez JM, Remesal J (2010) Estudios sobre el Monte Testaccio (Roma) V. Publicacions Universitat de Barcelona, Barcelona
Blázquez JM, Remesal J (2016) Estudios sobre el Monte Testaccio (Roma) V. Publicacions Universitat de Barcelona, Barcelona
Bonsor G (1931) The archaeological expedition along the Guadalquivir 1889–1901. Hispanic Society of America, New York
Bourgeon O (2016) Nuevos datos sobre la producción de ánforas Dressel 23 en el valle del Genil. In Járrega R, Bierni P (ed) Amphorae ex Hispania: paisajes de producción y consumo. III Congreso Internacional de la SECAH - Ex Officina Hispana (Tarragona, 10–13 diciembre 2014). Institut Català d'Arqueologia Clàssica, Tarragona, pp 334–346
Bourgeon O (2017) Baetican olive-oil trade under the Late Empire: new data on the production of Late Roman amphorae (Dressel 23) in the lower Genil valley. J Roman Archaeol 30:517–529
Buxeda J (1999) Alteration and contamination of archaeological ceramics: the perturbation problem. J Archaeol Sci 26:295–313
Buxeda J, Cau MA (2004) Annex I. Caracterització arqueomètrica de les produccions tardanes d'Iluro. In: Cela X, Revilla V (ed) La transició del municipium d'Iluro a Alarona (Mataró). Cultura material i transformacions d'un espia urbà entre els segles V i VII dC. Laietània 15 (monographic volume), Mataró, pp 449-498
Buxeda J, Kilikoglou V (2003) Total variation as a measure of variability in chemical data sets. In: Van Zelst L (ed) Patterns and process: a Festschrift in honor of Dr. Edward V. Sayre. Smithsonian Center for Materials Research and Education, Washington DC, pp 185–198
Carreras C (2014) Dressel 23. In: Roman amphorae: a digital resource. Archaeology data service, York. https://doi.org/10.5284/1028192.
Chic G (1985) Epigrafia anfórica de la Bética. 1, Las marcas impresas en el barro sobre ánforas olearias, Dressel 19, 20 y 23. Universidad de Sevilla, Sevilla
Chic G (2001) Datos para un estudio socioeconómico de la Bética. Marcas de alfar sobre ánforas olearias. Gráficas Sol, Écija
Chic G, García Vargas E (2004) Alfares y producciones cerámicas en la provincia de Sevilla. Balance y perspectivas. In Lagóstena L, Bernal D (ed) Figlinae Baeticae: talleres alfareros y producciones cerámicas en la Bética romana (ss. II a.C.-VII d.C.). Archaeopress, Oxford, pp 279-348
Corrales P, Compaña JM, Corrales M, Suárez J (2011) Salsamenta malacitano. Avances de un proyecto de investigación. Itálica, Revista de Arqueología Clásica de Andalucía 1:29–49
Costa BFO, Silva AJM, Ramalho A, Pereira G, Ramos Silva M (2012) X-ray compositional microanalysis and diffraction studies of Haltern 70 amphorae sherds. X-Ray Spectrom 41(2):69–74
Cultrone G, Rodriguez-Navarro C, Sebastian E, Cazalla O, De la Torre MJ (2001) Carbonate and silicate phase reactions during ceramic firing. Eur J Mineral 13:621–634
Étienne R, Mayet F (2004) L'huile hispanique. De Boccard, Paris
Fantuzzi L, Cau MA (2017) Investigating the provenance of the Baetican amphorae Dressel 23: new archaeometric evidence from Late Roman consumption centres. Mediterr Archaeol Archaeom 17(1): 47–68
García Ramos G, González García F, Fernández Veiguela D (1966) Arcillas cerámicas de Andalucía IV. Yacimientos terciarios de La Campiña, en la provincia de Córdoba. Bol Soc Esp Cerám Vidr 5(3):337–359
García Vargas E, Bernal D (2008) Ánforas de la Bética. In: Bernal D, Ribera A (eds) Cerámicas hispanorromanas: un estado de la cuestión. Servicio de Publicaciones de la Universidad de Cádiz, Cádiz, pp 661–687
González García F, García Ramos G (1964) Arcillas cerámicas de Andalucía I. Yacimientos de las vegas del Guadalquivir y Corbones en la provincia de Sevilla. Bol Soc Esp Cerám Vidr 3(5):481–502
González García F, García Ramos G (1965) Arcillas cerámicas de Andalucía II. Yacimientos de La Campiña, en la provincia de Sevilla. Bol Soc Esp Cerám Vidr 4(1):5–22
González Vílchez MC, González Rodríguez M, Aitlahsen Y (2001) Estudio arqueométrico de asas selladas de ánforas Dressel 20 del yacimiento arqueológico de La Catria (Lora del Río, Sevilla). In: Blázquez JM, Remesal J (eds) Estudios sobre el Monte Testaccio (Roma) II. Publicacions Universitat de Barcelona, Barcelona, pp 401–420
González-Delgado JA, Civis J, Dabrio CJ, Goy JL, Ledesma S, Pais J, Sierro FJ, Zazo C (2004) Cuenca del Guadalquivir. In: Vera JA (ed) Geología de España. Sociedad Geológica de España - Instituto Geológico y Minero de España, Madrid, pp 543–550
Grubessi O (1999) Progetto Testaccio, Roma. Uno studio archeometrico delle anfore Dressel 20. In: Blázquez JM, Remesal J (eds) Estudios sobre el Monte Testaccio (Roma) I. Publicacions Universitat de Barcelona, Barcelona, pp 365–424
Grubessi O, Conti L (1999) Progetto Testaccio. Studio archeometrico delle anfore Dressel 20: nota II. Confronto analitico tra i reperti spagnoli Tejarillo e La Catria e M. Testaccio. In: Blázquez JM, Remesal J (eds) Estudios sobre el Monte Testaccio (Roma) I. Publicacions Universitat de Barcelona, Barcelona, pp 513–542
Hein A, Tsolakidou A, Iliopoulos I, Momsen H, Buxeda J, Montana G, Kilikoglou V (2002) Standardisation of elemental analytical techniques applied to provenance studies of the archaeological ceramics: an inter laboratory calibration study. Analyst 127:542–553
IGME [Instituto Geológico y Minero de España] (1970) Mapa Geológico de España, E. 1:200.000, Sevilla, Hoja 75. Departamento de Publicaciones del Instituto Geológico y Minero de España, Madrid
IGME [Instituto Geológico y Minero de España] (1980) Mapa Geológico de España, E. 1:200.000, Córdoba, Hoja 76. Departamento de Publicaciones del Instituto Geológico y Minero de España, Madrid
Junta de Andalucía (1998) Mapa Geológico-Minero de Andalucía. Escala 1:400.000. Dirección General de Industria, Energía y Minas, Sevilla
Keay SJ (1984) Late Roman Amphorae in the Western Mediterranean. A tipology and economic study: the Catalan evidence. British Archaeological Reports, Oxford
Lemonnier P (1976) La description des chaînes opératoires: contribution a l'analyse des systèmes techniques. Techniques Cult 1:100–151
Lemonnier P (ed) (1993) Technological choices: transformation in material cultures since the Neolithic. Routledge, New York
Maggetti M (1982) Phase analysis and its significance for technology and origin. In: Olin JS, Franklin AD (eds) Archaeological ceramics. Smithsonian Institution Press, Washington DC, pp 121–133
Maggetti M, Neururer C, Ramseyer D (2011) Temperature evolution inside a pot during experimental surface (bonfire) firing. Appl Clay Sci 53:500–508
Manacorda D (1977) Le Anfore. In: Carandini A, Panella C (ed) Ostia IV: Le Terme del Nuotatore. Scavo dell'ambiente XVI e dell'area XXV. De Luca, Roma, pp 116–383
Murad E, Wagner U (1996) The thermal behaviour of an Fe-rich illite. Clay Miner 31:45–52
Polvorinos del Río AJ, Flores V, Tabales MA, Hernández MJ (2003) Caracterización y tecnología de materiales cerámicos romanos de los ss. I a III d.c procedentes del Hospital de las Cinco Llagas de Sevilla. Bol Soc Esp Cerám Vidr 42(2):93–99
Ponsich M (1974) Implantation rurale antique sur le bas-Guadalquivir, Tome 1. Casa de Velázquez, Madrid
Ponsich M (1979) Implantation rurale antique sur le bas-Guadalquivir, Tome 2. Casa de Velázquez, Madrid
Ponsich M (1991) Implantation rurale antique sur le bas-Guadalquivir, Tome 4. Casa de Velázquez, Madrid

Quinn PS (2013) Ceramic petrography. The interpretation of archeological pottery & related artefacts in thin section. Archaeopress, Oxford

Remesal J (1977) La economía oleícola bética: nuevas formas de análisis. Arch Esp Arqueol 50-51:87–142

Remesal J (1983) Transformaciones en la exportación del aceite bético a mediados del siglo III d.C. In: Producción y comercio del aceite en la antigüedad, II Congreso Internacional (Sevilla, 1982). Universidad Complutense, Madrid, pp 131–152

Remesal J (1989) Tres nuevos centros productores de ánforas Dressel 20 y 23. Los sellos de LVCIVS FABIVS CILO Ariadna 6:119–153

Remesal J (1991) El aceite bético durante el Bajo Imperio. In: González A, Fernández FJ, Remesal J (eds) Arte, sociedad, economía y religión durante el Bajo Imperio y la Antigüedad Tardía. Universidad de Murcia, Murcia, pp 355–361

Remesal J (2004) Alfares y producciones cerámicas en la provincia de Córdoba. Balance y perspectivas. In Lagóstena L, Bernal D (ed) Figlinae Baeticae: talleres alfareros y producciones cerámicas en la Bética romana (ss. II a.C.-VII d.C.). Archaeopress, Oxford, pp 349-361

Remolà JA (2000) Las ánforas tardo-antiguas en Tarraco (Hispania Tarraconensis). Publicacions Universitat de Barcelona, Barcelona

Reynolds P (1995) Trade in the Western Mediterranean, AD 400–700: the ceramic evidence. British Archaeological Reports, Oxford

Reynolds P (2010) Hispania and the Roman Mediterranean, AD 100–700. Ceramics and Trade, Duckworth, London

Roberts JP (1963) Determination of the firing temperature of ancient ceramics by measurement of thermal expansion. Archaeometry 6: 21–25

Rodríguez P (1997) Los hornos cerámicos del Faro de Torrox (Málaga). In: Figlinae Malacitanae: la producción de cerámica romana en los territorios malacitanos. Área de Arqueología de la Universidad de Málaga, Málaga, pp 271–303

Rodríguez Almeida E (1984) Il Monte Testaccio: ambiente, storia, materiali. Quasar, Roma

Romo A, Vargas JM (2001) Azanaque. Evidencias arqueológicas de un centro de producción anfórica. In: Congreso Internacional Ex Baetica Amphorae. Conservas, aceite y vino de la Bética en el Imperio Romano (Écija, Sevilla, 1998). Gráficas Sol, Écija, pp 405–417

Sala M (1984) Baetic Cordillera and Guadalquivir basin. In: Embleton C (ed) Geomorphology of Europe. Macmillan, London, pp 323–340

Schiffer MB, Skibo JM (1997) The explanation of artifact variability. Am Antiq 62(1):27–50

Serrano E (2004) Alfares y producciones cerámicas en la provincia de Málaga: balance y perspectivas. In Lagóstena L, Bernal D (ed) Figlinae Baeticae: talleres alfareros y producciones cerámicas en la Bética romana (ss. II a.C.-VII d.C.). Archaeopress, Oxford, pp 161-194

Sillar B, Tite M (2000) The challenge of 'technological choices' for materials science approaches in archaeology. Archaeometry 42(1): 2–20

Vera JA (1983) LA Cordillera Bética: las zonas externas. In: Comba JA (ed) Libro jubilar J.M. Ríos. Geología de España (Tomo II). Instituto Geológico y Minero de España, Madrid, pp 218–251

Viegas C (2011) A ocupação romana do Algarve: estudo do povoamento e economia do Algarve central e oriental no período romano. Centro de Arqueologia da Universidade de Lisboa, Lisboa

Whitbread IK (1989) A proposal for the systematic description of thin sections towards the study of ancient ceramic technology. In: Maniatis Y (ed) Archaeometry: proceedings of the 25th international symposium. Elsevier, Amsterdam, pp 127–138

Whitbread IK (1995) Appendix 3. The collection, processing and interpretation of petrographic data. In: Greek transport amphorae: a petrological and archaeological study. British School at Athens, Athens, pp 365–396